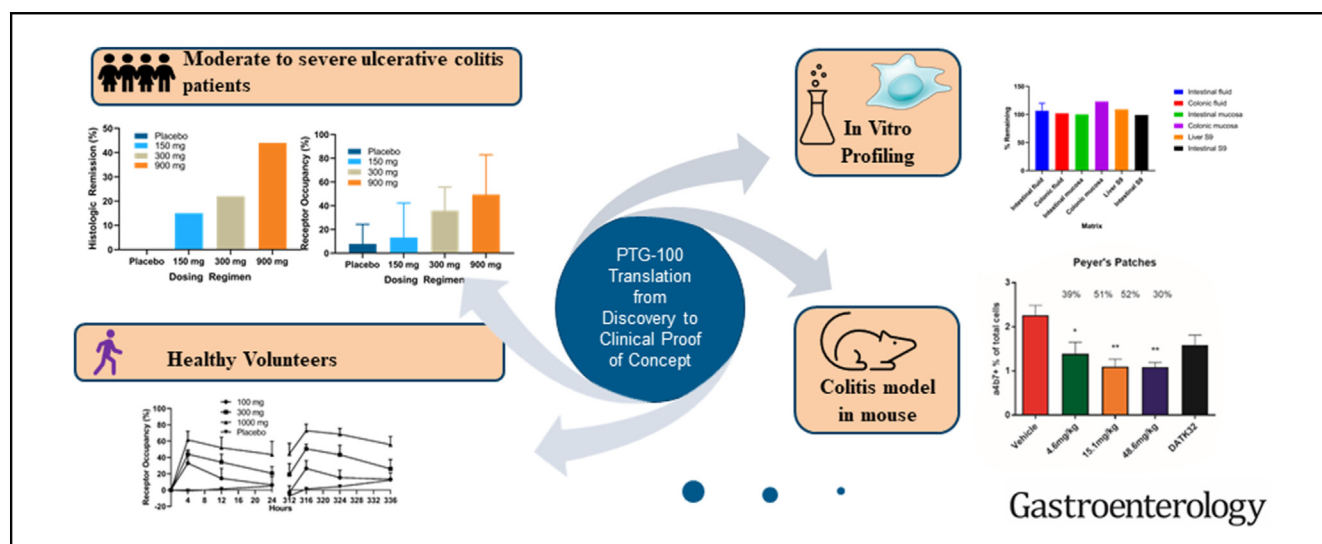


PTG-100, an Oral $\alpha 4\beta 7$ Antagonist Peptide: Preclinical Development and Phase 1 and 2a Studies in Ulcerative Colitis



William J. Sandborn,¹ Larry C. Mattheakis,² Nishit B. Modi,² David Pugatch,³ Brian Bressler,⁴ Scott Lee,⁵ Raj Bhandari,⁶ Bittoo Kanwar,⁷ Richard Shames,⁸ Geert D'Haens,⁹ Stefan Schreiber,¹⁰ Silvio Danese,¹¹ Brian Feagan,¹² Rish K. Pai,¹³ David Y. Liu,² and Suneel Gupta²

¹University of California–San Diego, San Diego, California; ²Protagonist Therapeutics, Inc, Newark, California; ³Finch Therapeutics, Inc, Somerville, Massachusetts; ⁴University of British Columbia, Vancouver, Canada; ⁵University of Washington, Seattle, Washington; ⁶Delta Research Partners, Bastrop, Louisiana; ⁷Applied Molecular Transport, San Francisco, California; ⁸Siolta, San Carlos, California; ⁹Faculty of Medicine, University of Amsterdam, Amsterdam, the Netherlands; ¹⁰University Hospital Schleswig-Holstein, Kiel University, Kiel, Germany; ¹¹Humanitas University, Humanitas Research Hospital, Milan, Italy; ¹²Western University, Pomona, California and Alimentiv, Inc, London, Ontario, Canada; and ¹³Mayo Clinic Arizona, Phoenix, Arizona



See editorial on page 1791.

BACKGROUND & AIMS: Oral therapies targeting the integrin $\alpha 4\beta 7$ may offer unique advantages for the treatment of inflammatory bowel disease. We characterized the oral $\alpha 4\beta 7$ antagonist peptide PTG-100 in preclinical models and established safety, pharmacokinetic/pharmacodynamic relationships, and efficacy in a phase 2a trial in patients with ulcerative colitis (UC). **METHODS:** In vitro studies measured binding properties of PTG-100. Mouse studies measured biomarkers and drug concentrations in blood and tissues. The phase 1 study involved healthy volunteers. In phase 2a, patients with moderate to severe active UC were randomized to receive PTG-100 (150, 300, or 900 mg) or placebo once daily for 12-weeks. **RESULTS:** PTG-100 potently and selectively blocks $\alpha 4\beta 7$. Oral dosing of PTG-100 in mice showed high levels of target

engagement and exposure in gut-associated lymphoid tissues. In healthy volunteers, PTG-100 showed dose-dependent increases in plasma exposure and blood target engagement. Although this phase 2a study initially did not meet the primary endpoint, a blinded reread of the endoscopy videos by a third party indicated clinical efficacy in conjunction with histologic remission at doses correlating with less than 100% receptor occupancy in peripheral blood. **CONCLUSIONS:** PTG-100 showed local gastrointestinal tissue target engagement and inhibition of memory T-cell trafficking in mice. It was safe and well tolerated in phase 1 and 2 studies. Phase 2a data are consistent with biological and clinical response and showed a dose response reflecting similar activities in preclinical models and healthy individuals. These data suggest that local gut activity of an oral $\alpha 4\beta 7$ integrin antagonist, distinct from full target engagement in blood, are important for efficacy and the treatment of UC. (ClinicalTrials.gov, Number NCT02895100; EudraCT, Number 2016-003452-75)

Keywords: Ulcerative Colitis; Inflammatory Bowel Disease; PROPEL Study; $\alpha 4\beta 7$ Integrin; PTG-100.

Ulcerative colitis (UC) is an inflammatory disease affecting the colon and rectum. It is a chronic condition with negative effects on quality of life, including symptoms of fatigue, depression, and diarrhea with blood and mucus discharge. Colectomy is a last resort option in the setting of refractory or fulminant disease, colorectal dysplasia, or cancer. Preclinical studies suggested that an important driver of this disease is effector memory T cells expressing the integrin $\alpha 4\beta 7$.^{1,2} Activated T cells expressing $\alpha 4\beta 7$ home to the inflamed gastrointestinal (GI) tract through binding of its specific ligand mucosal addressin cell adhesion molecule-1 (MAdCAM-1) expressed on endothelial venules, resulting in the capture, rolling, adhesion, and migration of the T cells through the vascular wall to the underlying mucosa.³ Blocking this interaction by vedolizumab has been shown to be clinically efficacious in UC⁴ and Crohn's disease (CD).⁴⁻⁶ Vedolizumab is a parenterally administered humanized monoclonal antibody that binds to the $\alpha 4\beta 7$ integrin heterodimer on the surface of T cells and prevents their trafficking into the GI tract. It has been assumed that vedolizumab's site of action is solely within the peripheral blood, and therefore, 100% receptor occupancy (RO) of $\alpha 4\beta 7$ by vedolizumab in the blood is sufficient for clinical efficacy.

Studies have shown, however, an apparent lack of correlation between blood RO and clinical efficacy for vedolizumab. Population pharmacokinetic (PK) and pharmacodynamic (PD) modeling based on the GEMINI 1 and GEMINI 2 studies indicated the vedolizumab serum concentration at half-maximum effect (EC_{50}) at 0.093 $\mu\text{g/mL}$, which suggests that complete receptor saturation is reached at a vedolizumab serum concentration of approximately 1 $\mu\text{g/mL}$, a concentration considered subtherapeutic for clinical efficacy.^{4,5,7} Exposure efficacy data at week 6 indicated that vedolizumab concentrations of ≤ 17.1 $\mu\text{g/mL}$ in patients with UC in GEMINI 1 and ≤ 16 $\mu\text{g/mL}$ in patients with CD in GEMINI 2 during induction were associated with clinical remission rates similar to placebo. These observations suggest that complete saturation of $\alpha 4\beta 7$ in the blood may not be sufficient for clinical efficacy of vedolizumab.⁸

Similar observations were made from a prospective study in patients with inflammatory bowel disease showing that the median trough levels of vedolizumab at week 6 were higher in patients in clinical remission (40.2 $\mu\text{g/mL}$) than in patients with active disease (29.7 $\mu\text{g/mL}$), despite complete saturation of $\alpha 4\beta 7$ expressed on peripheral blood memory T cells at both trough concentrations.⁹ In the same study, analysis of intestinal $CD3^+CD45RO^+$ memory T cells also showed $>94\%$ saturation of $\alpha 4\beta 7$ for responders and nonresponders. In another prospective study in patients with IBD, vedolizumab trough levels were also sufficient for complete saturation of $\alpha 4\beta 7$ among responders (41.8 $\mu\text{g/mL}$) and nonresponders (39.3 $\mu\text{g/mL}$).¹⁰ Together, these results suggest that vedolizumab requires additional

WHAT YOU NEED TO KNOW

BACKGROUND AND CONTEXT

Oral therapies targeting the integrin $\alpha 4\beta 7$ locally in the gastrointestinal tissue may offer unique advantages for the treatment of inflammatory bowel disease.

NEW FINDINGS

PTG-100, an oral $\alpha 4\beta 7$ antagonist with high gastrointestinal exposure and limited systemic exposure, showed efficacy in conjunction with histologic remission at doses correlating with less than 100% receptor occupancy in peripheral blood.

LIMITATIONS

This phase 2a study in a limited number of participants initially did not meet the primary endpoint, underwent blinded reread of the endoscopy videos, and subsequently showed dose-dependent effects in PTG-100 recipients versus those receiving placebo.

IMPACT

The consistent preclinical biological and phase 2a data suggest that local gut activity of an oral $\alpha 4\beta 7$ integrin antagonist, distinct from full target engagement in blood, may be important for efficacy and the treatment of ulcerative colitis.

mechanisms besides peripheral blood $\alpha 4\beta 7$ saturation to achieve clinical efficacy.

PTG-100, unlike vedolizumab, is an oral $\alpha 4\beta 7$ peptide antagonist that has high GI exposure with limited absorption and systemic exposure. Here, we describe PTG-100's preclinical development and its efficacy, safety, PK, and PD including RO in healthy volunteers and patients with moderate to severe UC.

Methods

Preclinical Studies

Oral pharmacokinetic and pharmacodynamic studies in mice. These procedures are described in the [Supplementary Methods](#). Briefly, fasted female C57BL/6 mice (Charles River Laboratories), 8–10 weeks old, were orally dosed with PTG-100 (30 mg/kg). Vehicle was 50 mmol/L sodium phosphate buffer with a pH of 7.4. For PD studies, animals were killed 1 hour postdose, and terminal blood or plasma

Abbreviations used in this paper: CD, Crohn's disease; C_{max} , maximum concentration; DMC, data monitoring committee; DSS, dextran sulfate sodium; EC_{50} , half maximal effective concentration; GALT, gut-associated lymphoid tissues; GI, gastrointestinal; IA, interim analysis; IBD, inflammatory bowel disease; IC_{50} , half maximal inhibitory concentration; MAdCAM-1, mucosal addressin cell adhesion molecule-1; MLN, mesenteric lymph node; PBMC, peripheral blood mononuclear cell; PD, pharmacodynamic; PK, pharmacokinetic; RE, receptor expression; RO, receptor occupancy; SAE, serious adverse event; T_{max} , time to maximum concentration; UC, ulcerative colitis.

Most current article

© 2021 by the AGA Institute. Published by Elsevier Inc. This is an open access article under the CC BY-NC-ND license (<http://creativecommons.org/licenses/by-nc-nd/4.0/>).

0016-5085

<https://doi.org/10.1053/j.gastro.2021.08.045>

samples were collected for RO and PTG-100 concentration analysis, respectively. Cell suspensions from the Peyer's patches were prepared by mechanical dissociation for flow analysis. For the PK study, terminal blood and tissue samples were collected at 0.25, 0.5, 1, 2, 4, 8, 12, and 24 hours postdose and processed to plasma and tissue homogenates. Plasma and tissue PTG-100 concentrations were determined by liquid chromatography–tandem mass spectrometry.

T-cell trafficking in a mouse dextran sulfate sodium colitis model. Colitis was induced in C57Bl/6 male mice, 6–8 weeks old (Charles River Laboratories), by exposure to 3% dextran sulfate sodium (DSS)–treated drinking water from day 0 to day 5. Starting on day 0, mice were given twice-daily oral doses of either vehicle control or PTG-100. DATK32 (a monoclonal antibody against mouse integrin $\alpha_4\beta_7$) (25 mg/kg) was administered by intraperitoneal injection on days 0, 3, and 6. PTG-100 was also administered in the drinking water. The volume of consumed drinking water and dose by oral gavage was used to determine the total indicated dose. Mice were killed on day 9 approximately 4 hours after the final dose of PTG-100. Spleen, Peyer's patches, mesenteric lymph nodes (MLNs), and whole blood were collected from all animals and processed for flow cytometry analysis of α_4 and β_7 expression on T helper memory cells, as described in the [Supplementary Methods](#).

Clinical Studies

Phase 1 first-in-human healthy volunteers. A randomized, double-blind, placebo-controlled phase 1 study including 78 healthy male volunteers was conducted to evaluate the safety, tolerability, PK, and PD of PTG-100. The primary objective of the study was to determine the safety and tolerability of single- and multiple-dose administration of PTG-100. Secondary objectives were to assess the plasma PK and blood PD (RO and $\alpha_4\beta_7$ receptor expression [RE] on peripheral blood memory T cells). The study consisted of a single ascending dose and multiple ascending dose administration (once-daily dosing for 14 days up to a maximum dose of 1000 mg) of PTG-100 in a liquid phosphate buffer formulation. Inclusion and exclusion criteria are detailed in the [Supplementary Methods](#). Blood sampling for PK and PD assessments were obtained for up to 48 hours after the single dose and for up to 36 hours after the last dose in the multiple-dose phase. Non-compartmental PK analyses were conducted using Phoenix WinNonlin, version 8.3 (Certara).

Phase 2a randomized, double-blind, placebo-controlled study of PTG-100. Study population. This phase 2a study of PTG-100 (PROPEL) included male and female participants aged 18–80 years with moderate to severe UC, defined as a Mayo Score of 6 to 12 at baseline with a centrally read endoscopy score of ≥ 2 . Participants must have been diagnosed with UC for at least 2 months before screening and have had an inadequate response, loss of response, or intolerance to at least 1 of the following medications: corticosteroids, immunomodulators, and tumor necrosis factor alpha antagonists. Individuals with CD, indeterminate colitis, or presence or history of the following were excluded: fistula, toxic megacolon, abdominal abscess, symptomatic colonic stricture or stoma, past or imminent risk of colectomy, and colonic dysplasia. Infection-related exclusions included known immunodeficiency, current bacterial or parasitic pathogenic enteric

infection (including *Clostridium difficile*), hepatitis B or C, human immunodeficiency virus, hospitalization or administration of intravenous antimicrobial therapy within 6 months, opportunistic infection within 6 months, infection requiring antimicrobial therapy within 2 weeks, and a history of ≥ 1 episode of herpes zoster or any episode of disseminated zoster. Other major exclusion criteria included presence of clinically significant or uncontrolled major medical disorders that might confound results or pose additional risk to participants.

Study design. The PROPEL study was a global, randomized, double-blind, placebo-controlled, multicenter, 2-stage adaptive trial in patients with moderate to severe active UC. The study was conducted with 103 sites between January 10, 2017, and March 23, 2018. Matching PTG-100 (150-mg or 300-mg capsule) and placebo capsules identical in appearance (manufactured by Catalent) were provided to participants according to the randomization schedule. Treatment duration was 12 weeks in the induction stage of the study. Participants were randomized via an interactive web response system (1:1:1:1) to 3 PTG-100 once-daily doses (150 mg, 300 mg, and 900 mg) or placebo, with approximately 60 participants planned per arm, for an overall planned study population of 240. Participant enrollment occurred in 2 stages relative to an interim analysis (IA) performed by an unblinded, independent data monitor committee (DMC). The purpose of the IA was to conduct a futility analysis according to prespecified criteria and, if nonfutile, to identify which study arms provided optimal data to select 1 (or 2) PTG-100 dose levels and placebo to continue enrolling participants to the most informative and effective dose arms. After the IA, additional participants were to be randomized equally (1:1 or 1:1:1, as appropriate) to the selected doses of PTG-100 and placebo. The schematic of the study design is displayed in [Supplementary Figure 1](#).

The study was overseen by Protagonist Therapeutics and conducted by clinical investigators. The DMC was independent from the sponsor and reviewed unblinded safety and efficacy data. The study protocol was reviewed and approved by the institutional review boards at the participating study sites. Study participants provided informed consent. The study was conducted in compliance with the Declaration of Helsinki and the International Conference on Harmonisation Guidelines for Good Clinical Practice. All authors had access to the study data and reviewed and approved the final study manuscript.

Study endpoints. The primary efficacy endpoint was the proportion of participants receiving PTG-100 with clinical remission at week 12 compared with placebo. Clinical remission was defined based on the 3-component Mayo Clinic Score¹¹ as follows, using the subscores of stool frequency, rectal bleeding, and endoscopy: (1) stool frequency subscore of 0 or 1 with a prespecified change of 1 or more from baseline, (2) rectal bleeding subscore of 0, and (3) endoscopy subscore of 0 or 1 (modified from the original description such that a score of 1 does not include friability). Secondary endpoints were proportion of participants with endoscopic improvement (endoscopic subscore of 0 or 1) at week 12; clinical response (defined as at least a 1-point and 30% reduction from baseline in rectal bleeding and stool frequency subscores, respectively) at week 12; mean change in endoscopy subscore; mean change in rectal bleeding and stool frequency subscores from baseline to weeks 2, 4, 6, 8, 10, 12, and 16; proportion of participants with endoscopic remission (endoscopic subscore of 0) at week

12; mean change in Mayo Score from baseline to week 12; mean change in partial Mayo Score from baseline to weeks 2, 4, 8, 12, and 16; mean change in fecal calprotectin levels from baseline to weeks 6 and 12; mean change in Inflammatory Bowel Disease Questionnaire score¹² from baseline to week 12; proportion of participants developing antidrug antibodies; and the frequency and type of adverse events.

Interim analysis. An unblinded IA was performed by the independent DMC after 65 participants had been dosed and completed 12 weeks of dosing or terminated early (stage 1). The criteria for futility were predefined in the DMC charter and were based on achieving at least 10% conditional power to achieve the primary endpoint. Based on the prespecified criteria, the trial was declared futile by the DMC, and further recruitment to the trial was discontinued based on the futile outcome.

Study assessments. Participants underwent a screening period of up to 35 days. Participants were assessed on day 1 (baseline) and at weeks 2, 4, 6, 8, and 12. Flexible sigmoidoscopy with colonic biopsy was performed at screening and at week 12. Biopsy specimens were taken from the most inflamed area of the colon while avoiding necrotic areas of ulcerated mucosa or suture sites in patients with previous colonic resection. Biopsy specimens were to be obtained from the same area at baseline and at week 12. For each endoscopy procedure video, the Mayo endoscopic subscore was determined by 1 central reader blinded to treatment assignment. Histologic disease activity from colonic biopsy samples was assessed using Geboes score and Robarts Histopathology Index by a pathologist blinded to study treatment.

Adverse events and use of concomitant medications were recorded through 12 weeks. Blood samples were obtained at each visit for clinical chemistry and hematology as well as measurement of C-reactive protein, and stool samples were obtained at baseline and weeks 6 and 12 for fecal calprotectin (central laboratory: Covance, Inc).

Clinical pharmacokinetics. Blood samples for the measurement of PTG-100 plasma concentrations were collected predose and at 1, 2, and 4 hours after the first dose and after the last dose of PTG-100. In addition, predose samples were collected at week 2, 4, 6, and 8. Plasma concentrations of PTG-100 were determined using a validated liquid chromatography–tandem mass spectrometry method. Non-compartmental PK analyses were conducted using Phoenix WinNonlin, version 8.3 (Certara).

Clinical pharmacodynamics. PD assessments of blood RO and integrin expression were done at most visits. Heparinized whole blood was stained with each of 2 panels of antibodies to evaluate the extent of $\alpha 4\beta 7$ receptor occupancy, expression, and abundance of circulating $\alpha 4\beta 7^+$ lymphocyte subsets within the memory $CD4^+$ T cells, naive $CD4^+$ T cells, and B cells. RO and RE methods are described in the [Supplementary Methods](#).

Histopathology and immunohistochemistry of colon biopsy samples. Tissue blocks were cut and stained and slides were prepared and scored by a pathologist according to the method of Pai et al.¹³ For immunohistochemistry staining of PTG-100, slides from 10 patients at screening and week 12 (900-mg dose cohort) were stained with an 1/1800 dilution of a rabbit polyclonal anti-PTG-100 affinity purified antibody. Staining specificity was confirmed by costaining with an excess of PTG-100 blocking peptide. Slide images were scanned and evaluated by a pathologist.

Results

Preclinical Studies

PTG-100 binding properties. PTG-100 potently and selectively blocked adhesion of cells expressing $\alpha 4\beta 7$ integrin to MAdCAM-1. For $CD4^+$ memory T cells isolated from human peripheral blood mononuclear cell (PBMC) donors, PTG-100 blocked adhesion to MAdCAM-1 (half maximal inhibitory concentration [IC_{50}], 1.7 ± 0.8 nmol/L), but not adhesion to vascular cell adhesion molecule-1 (VCAM-1) (IC_{50} , $>100,000$ nmol/L) or intracellular adhesion molecule-1 (ICAM-1) (IC_{50} , $>100,000$ nmol/L) ([Supplementary Table 1](#)). Similar potency and selectivity were observed using transformed cell lines. The PTG-100 IC_{50} for blocking adhesion of the human B-cell lymphoblastoid RPMI8866 or mouse T-cell TK1 cell lines expressing $\alpha 4\beta 7$ to human MAdCAM-1 is 0.72 ± 0.28 nmol/L and 0.50 ± 0.02 nmol/L, respectively. Selectivity was also shown using human Jurkat cells expressing $\alpha 4\beta 1$. PTG-100 was inactive at blocking adhesion of Jurkat cells to VCAM-1 at the maximum concentration tested (IC_{50} , $>100,000$ nmol/L). Together, these results indicate that, like vedolizumab, PTG-100 is specific for $\alpha 4\beta 7$ and does not block the $\alpha 4\beta 1$ integrin.

We also compared the $\alpha 4\beta 7$ binding kinetics of PTG-100 and vedolizumab by surface plasmon resonance. The sensorgrams showed the calculated dissociation constant (K_D) for PTG-100 (15.4 ± 3 nmol/L) is 3.8-fold lower than for vedolizumab (59.5 ± 5 nmol/L), and its half-life of dissociation from the $\alpha 4\beta 7$ integrin protein under activated conditions is 11 hours, compared to 0.7 hours for vedolizumab ([Supplementary Table 2](#)). Schild analysis using an enzyme-linked immunosorbent assay to measure the binding of MAdCAM-1 to $\alpha 4\beta 7$ indicates that PTG-100 antagonism is a simple competitive mechanism, reversible, and surmountable by increasing MAdCAM-1 concentration ([Supplementary Figure 2](#)). These data suggest that PTG-100 and MAdCAM-1 may bind to the same site on $\alpha 4\beta 7$.

Binding of $\alpha 4\beta 7$ to MAdCAM-1 is dependent on the conformational and activation states of the integrin.¹⁴ PTG-100 binds specifically to the activated state of $\alpha 4\beta 7$. Activation can be achieved either by including manganese chloride ($MnCl_2$) in the binding assays or culturing PBMCs with anti-CD3, interleukin 2, and retinoic acid under physiologic concentrations of Mg^{2+} . Retinoic acid is a key signal for imprinting GI homing specificity on T cells.¹⁵ Binding of PTG-100 to $\alpha 4\beta 7$ integrin expressed on PBMCs is similar in the presence of $MnCl_2$ or after activation by retinoic acid ([Supplementary Figure 3](#)), indicating that PTG-100 binding occurs under physiologic conditions.

The binding specificities of PTG-100 and vedolizumab were also compared by flow cytometry analysis of human whole blood. The data showed that PTG-100 and vedolizumab have nearly identical binding selectivity against 10 different cell types of lymphoid and myeloid lineage,¹⁶ despite PTG-100 being a peptide approximately 50 times smaller than the antibody ([Supplementary Table 3](#)).

PTG-100 also induces near-complete internalization of the $\beta 7$ integrin expressed on human $CD4^+$ memory T cells. Integrin $\beta 7$ internalization was detectable at as early as 1 hour but was most pronounced and nearly complete at 24 hours (Supplementary Figure 4).

PTG-100 stability in gastrointestinal fluids. Although PTG-100 is a peptide, a portion of it contains nonnatural amino acids, which allows it to be resistant to the proteolytic and reducing environment of the intestinal tract. In composite GI fluid from 3 human cadaver donors, there was no measurable degradation of PTG-100 after 24 hours of incubation. It is also stable after 6-hour incubations in simulated gastric fluid containing porcine pepsin and in rat preparations of colonic fluid, intestinal mucosa, and colonic mucosa. Some degradation was observed in simulated intestinal fluid from pig containing pancreatic enzymes (Supplementary Table 4). PTG-100 was also stable for at least 6 hours and 1 hours in rat liver S9 and human intestinal S9 fractions, respectively (Supplementary Table 4).

PTG-100 pharmacokinetic and pharmacodynamic studies in mice. Oral dosing of PTG-100 showed it to be mostly restricted to the gut, with higher exposure levels in the gut-associated lymphoid tissues (GALT) compared to plasma. A single dose of PTG-100 (30 mg/kg) in mice resulted in higher maximum concentrations (C_{max}) in the Peyer's patches, MLNs, small intestine, and colon compared to plasma (Supplementary Table 5). Concentrations within specific intestinal subregions of the duodenum, jejunum, ileum, and cecum were not measured. Although oral dosing of PTG-100 results in some plasma exposure, the vast majority of absorbed drug is retained within the GI tissues.

To confirm that higher drug concentrations in the GALT result in higher levels of target engagement in colonic tissue relative to blood, we repeated the mouse study at the same dose (30 mg/kg) and collected whole blood and single-cell suspensions from the Peyer's patches for RO analysis by flow cytometry and plasma for PK. At 1-hour postdose, the percent RO of $\alpha 4\beta 7$ expressed on $CD4^+$ effector memory T cells in the Peyer's patches was 92%, compared to 15% for whole blood. Drug concentrations were also higher in Peyer's patches (37 nmol/L) compared to plasma (3.3 nmol/L) (Supplementary Figure 5). Therefore, oral dosing of PTG-100 results in high levels of target engagement in the GALT.

We also measured the blood PD responses of PTG-100 repeat dosing in healthy mice. Mice were dosed with PTG-100 at 8.5, 25, and 85 mg/kg twice daily for 14 days, and blood was collected at 4, 12, and 24 hours postdose on day 14. Supplementary Figure 6A shows that RO in blood was dose dependent. At 4 hours postdose, blood RO was 32%, 39%, and 71% at 8.5, 25, and 85 mg/kg, respectively, and higher at 4 hours and 12 hours postdose compared to 24 hours postdose for all dose groups. Supplementary Figure 6B shows that down-regulation of $\alpha 4\beta 7$ integrin RE was also dose and time dependent. Down-regulation at the 8.5, 25, and 85 mg/kg twice daily doses at 4 hours postdose was 45%, 47%, and 56%, respectively, relative to the vehicle controls. This down-regulation of $\alpha 4\beta 7$ in mouse is consistent with the observed integrin internalization in

human PBMCs (Supplementary Figure 4) and suggests that PTG-100 may block $\alpha 4\beta 7$ adhesion to MadCAM-1 by either steric blockade or loss of $\alpha 4\beta 7$ expression through integrin internalization.

PTG-100 effects on T-cell trafficking in colitis mice. We next investigated the effects of PTG-100 dosing on T-cell trafficking in a 9-day DSS mouse colitis model. PTG-100 dosing was a combination of oral gavage and in drinking water, and the average total daily doses were 4.6, 15.1, and 48.6 mg/kg. At the end of the study, the normalized cell numbers of $\alpha 4\beta 7^+$ memory T cells in the MLNs, Peyer's patches, and blood were measured by flow cytometry. We included a control group dosed with the systemic mouse anti- $\alpha 4\beta 7$ antibody DATK32 (25 mg/kg intraperitoneally every 3 days). This dose of DATK32 has been shown to be efficacious in an adoptive T-cell transfer mouse colitis model,¹⁷ and mouse PK studies showed that this dose of DATK32 is sufficient for complete saturation of circulating $\alpha 4\beta 7^+$ T cells (data not shown). In contrast, PTG-100 at these dose levels results in higher levels of target engagement in the GALT compared to blood (Supplementary Figure 5). Despite these differences in blood target engagement, both PTG-100 and DATK32 significantly reduced T-cell trafficking to the MLNs and Peyer's patches and diverted these cells to the blood (Figure 1). In conclusion, PTG-100 dosing results in higher levels of target engagement in the GALT compared to blood, yet it affects T-cell trafficking like a systemic antibody, perhaps because of additional local effects in the intestinal tract.

In a separate 15-day mouse DSS-induced colitis model, we measured the effects of oral PTG-100 dosing on the number of $\beta 7^+$ cells in the distal colon using immunohistochemistry. The results showed that at all doses ranging from 6–55 mg/kg/day, PTG-100 significantly reduced the number of $\beta 7^+$ cells that infiltrated the mouse distal colon (Supplementary Figure 7).

Phase 1 First-in-Human Study in Healthy Volunteers

As predicted based on preclinical studies, PTG-100 plasma levels were low and increased only modestly with single and multiple dosing. Mean peak plasma concentration (C_{max}) and area under the curve to the last sampling point (AUC_t) increased with increasing PTG-100 dose after a single dose. There was a small increase in half-life with dose, ranging from 3.1 hours at 100 mg to 5.9 hours at 1000 mg. Assessment of dose proportionality using a power model indicated that the 90% confidence interval for the exponent included unity for both C_{max} and AUC_t , suggesting a dose-proportional increase (Supplementary Table 6).

After once-daily dosing of PTG-100, peak concentrations occurred 2–4 hours after dosing, and mean peak plasma concentrations increased with dose on day 1 and day 14 (Table 1). There was minimal accumulation after once-daily dosing, as noted by the similar C_{max} values on day 1 and day 14.

The mean recovery values of PTG-100 in urine over 24 hours for the 300- and 1000-mg dose groups were 0.067%

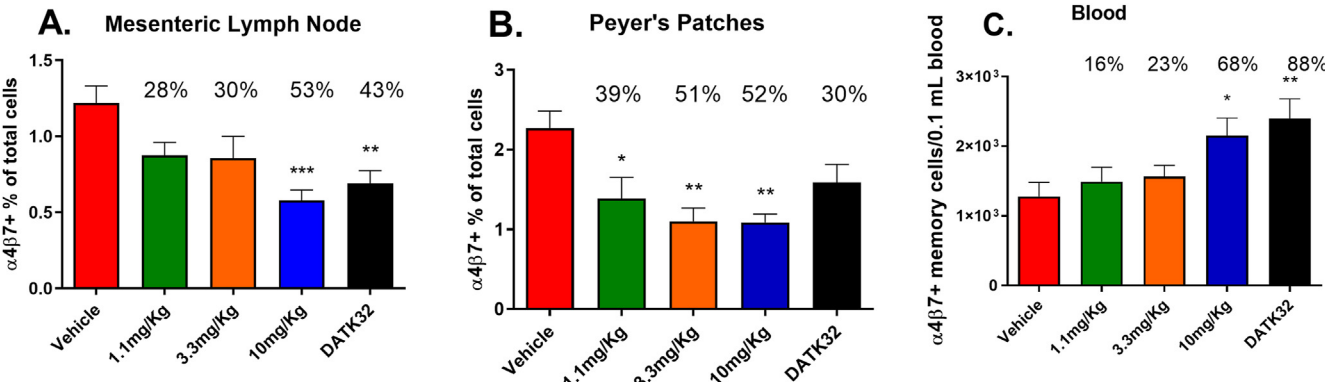


Figure 1. PTG-100 affects trafficking of $\alpha 4\beta 7$ + memory T cells in colitis mice within (A) MLNs, (B) Peyer's patches, and (C) blood compartments. Data are presented as mean percentage \pm standard deviation. For blood, the absolute number of $\alpha 4\beta 7$ + memory T cells is measured from 100 μ L of blood. PTG-100 total dose units are mg/kg/day based on oral gavage and consumed drinking water. DATK32 was dosed 25 mg/kg intraperitoneal once every 3 days. Values above bars are the percent decrease relative to vehicle control. Statistical analysis was performed via 1-way analysis of variance (ANOVA) with Dunnett multiple comparison test. * $P < .05$; ** $P < .01$; *** $P < .001$.

and 0.053%, respectively. Fecal recovery values of intact PTG-100 for the 300- and 1000-mg dose groups were 7.6% and 15.8%, respectively, confirming that the drug was stable throughout the GI tract. PTG-100 was well tolerated, and there were no serious adverse events (SAEs) or dose-limiting toxicities reported in healthy participants.

Similar to observations in the healthy and colitis mice studies, PTG-100 blood percent RO on CD4⁺ memory $\alpha 4\beta 7$ + T cells increased in a dose-dependent manner in both the single- and multiple-ascending-dose cohorts. These levels persisted to 24 hours with once-daily dosing, indicating that a sustained level of target engagement was achieved with once-daily dosing over 14 days (Supplementary Figure 8). Consistent with observations in the mouse models, $\alpha 4\beta 7$ expression (%RE) on CD4⁺ memory T cells (eg, receptor down-regulation) was reduced after single and multiple dosing. At 12 and 24 hours after 14 days of dosing of PTG-100, both blood percent RO and percent RE at the 300-mg human dose were comparable to levels in healthy mice at an equivalent dose (50 mg/kg/day) after 14 days of dosing (Supplementary Table 7).

In conclusion, PTG-100 was well tolerated after single and multiple dose administration in healthy volunteers up to a maximum dose of 1000 mg. The PK and PD data indicate that oral administration of PTG-100 results in low plasma levels with evidence of sustained target engagement and pharmacologic activity in peripheral blood CD4⁺ memory T cells in a dose- and time-dependent manner.

Phase 2 Randomized, Double-Blind, Placebo-Controlled Study of PTG-100

Phase 2a study demographics. A total of 98 participants received the study drug (PTG-100 or placebo). Of these 98 participants, 25 participants received placebo, 25 participants received PTG-100 150 mg, 25 participants received PTG-100 300 mg, and 23 participants received PTG-100 900 mg. Fifty-eight (59.2%) participants completed the study; 40 (40.8%) participants discontinued the study. Details regarding patient disposition are provided in Supplementary Figure 9. The demographic and baseline characteristics of enrolled participants are shown in Table 2.

Table 1. Summary of Phase 1 Multiple-Dose PK After Once-Daily Dosing of PTG-100 (n = 24 participants)

PTG-100 Dose	n	Day 1			Day 14		
		C_{max} , ng/mL	T_{max} , h, median (range)	AUC_{24} , ng·h/mL	C_{max} , ng/mL	T_{max} , h, median (range)	AUC_{24} , ng·h/mL
100 mg	8	1.70 \pm 0.97	2.0 (1–4)	12.5 \pm 6.7 ^a	1.80 \pm 1.1	2.0 (1–2)	19.1 ^b
300 mg	8	4.60 \pm 2.2	3.0 (2–8)	36.0 \pm 11 ^a	4.37 \pm 2.1	2.0 (1–12)	46.8 \pm 17 ^c
1000 mg	8	10.8 \pm 6.3	3.0 (1–4)	111 \pm 80	10.0 \pm 2.3 ^d	2.0 (1–8) ^d	130 \pm 45 ^d

^an = 4.
^bn = 1.
^cn = 6.
^dn = 7.

Table 2. Phase 2a Study (PROPEL) Demographics and Baseline Characteristics (N = 98 Participants)

Characteristics	Placebo	PTG-100 150 mg	PTG-100 300 mg	PTG-100 900 mg	Total
Age, y					
n	25	25	25	23	98
Mean (SD)	42.2 (14.9)	45.2 (13.8)	43.8 (17.0)	40.6 (14.1)	43.0 (14.9)
Sex, n (%)					
n	25	25	25	23	98
Male	15 (60.0)	18 (72.0)	10 (40.0)	9 (39.1)	52 (53.1)
Female	10 (40.0)	7 (28.0)	15 (60.0)	14 (60.9)	46 (46.9)
Race, n (%)					
n	25	25	25	23	98
White	23 (92.0)	19 (76.0)	23 (92.0)	22 (95.7)	87 (88.8)
Asian	0	4 (16.0)	1 (4.0)	0	5 (5.1)
Black or African American	2 (8.0)	2 (8.0)	0	1 (4.3)	5 (5.1)
Other	0	0	1 (4.0)	0	1 (1.0)
Weight, kg					
n	25	25	25	23	98
Mean (SD)	69.5 (16.1)	77.8 (16.3)	70.7 (15.4)	72.3 (19.1)	72.6 (16.8)
BMI, kg/m ²					
n	25	25	25	23	98
Mean (SD)	23.7 (4.7)	25.7 (4.7)	24.5 (5.2)	23.9 (4.5)	24.5 (4.8)
Total Mayo score					
n	25	25	25	23	98
Mean (SD)	8.2 (1.2)	8.1 (1.4)	8.9 (1.5)	8.2 (1.5)	8.4 (1.4)
Stool frequency subscore, n (%)					
n	25	24	25	23	98
Normal	1 (4.0)	0	1 (4.0)	0	2 (2.0)
1 or 2 stools/day more than normal	5 (20.0)	4 (16.0)	3 (12.0)	7 (30.4)	19 (19.4)
3 or 4 stools/day more than normal	9 (36.0)	8 (32.0)	7 (28.0)	10 (43.5)	34 (34.7)
>4 stools/day more than normal	10 (40.0)	12 (48.0)	15 (56.0)	6 (26.1)	42 (42.9)
Rectal bleeding subscore					
n	25	24	25	23	97
Mean (SD)	1.5 (0.7)	1.4 (0.9)	1.6 (0.8)	1.3 (0.7)	1.5 (0.8)

Phase 2a study efficacy. The IA was performed on data from 65 enrolled participants. Based on the prespecified criteria, the trial was declared futile by the DMC, and further recruitment of new participants to the trial was discontinued based on the futile outcome. However, upon unblinding of the interim data after the futile outcome, an unusually high placebo remission rate of 24% was observed, which is approximately 4 times higher than what had been observed in similar trials using centralized endoscopic reading ([Supplementary Table 8](#)).^{4,18–21}

After the discovery of this finding, we conducted a systematic evaluation of the high placebo rate. Occurrence of operational errors, such as misrandomization of participants or study drug or high rates of protocol deviations, were ruled out. It was confirmed that the target population was consistent with other trials and at baseline had moderate to severe disease with regard to prior UC history and current disease activity. Upon initial evaluation of the endoscopic reads of the placebo remitters, we noted that some specific errors were made by the central read clinical

research organization in applying scoring criteria to the individual endoscopy videos. (For example, in certain cases, the presence of mucosal friability was inappropriately scored as a 1 and not a 2.) Blinded endoscopy rereads of participants in the futility data set (n = 65) and the full futility dataset—that is, all participants who completed or terminated the study early before the futility announcement (n = 83)—were conducted by expert gastroenterologists affiliated with a second independent clinical research organization (Alimentiv). The results of the blinded reread of the endoscopies of the 65 participants included in the futility assessment is presented in [Supplementary Table 9](#). The endoscopy rereads confirmed that the trial would not have met futility and would have continued as planned. The reread of the full data set (n = 83) ([Table 3](#)) showed a low placebo rate of 1/21 (4.8%) for clinical remission, in line with historical data for such trials in UC and evidence of clinical remission in the treatment groups, specifically at the 300-mg (2/21, 9.5%) and 900-mg (3/19, 15.8%) doses. There was also evidence of endoscopic improvement as

Table 3. Overall Summary of Efficacy Endoscopy Reread

PTG-100 Dose, mg	Clinical Remission, n/total (%)	Endoscopic Improvement, n/total (%) ^a
150	2/22 (9.1)	2/22 (9.1)
300	2/21 (9.5)	3/21 (14.3)
900	3/19 (15.8)	3/19 (15.8)
Placebo	1/21 (4.8)	1/21 (4.8)

NOTE. Full data set, n = 83 participants.

^aEndoscopic improvement was defined as an endoscopic subscore of 0 or 1 of the Mayo score.

defined as an endoscopic subscore of 0 or 1 on the Mayo score at the 300-mg (3/21, 14.3%) and 900-mg (3/19, 15.8%) doses compared to placebo (1/21, 4.8%).²²

An important lesson from this study was to implement continued random audits and to ensure interreader agreement in the scoring during the conduct of studies involving UC. Although rigorous training and good interreader correlation can be demonstrated before the initiation of a study, there can be apparent drift in interreader agreement during the course of a study that may not be evident in time for remediation. These observations show the need for continued monitoring during the course of a clinical study involving central reading.

In addition, supportive evidence for a treatment effect was noted on histopathology analysis of the colon biopsy samples. Using the Robarts Histopathologic Index, a definition of histologic remission was defined as a week 12 score of ≤ 3 (with an absence of neutrophils and no erosions or ulcerations) among participants who had a score of >3 at baseline.¹³ Figure 2 shows dose-dependent evidence of histologic remission at week 12 up to 7 of 16 (44%) for the

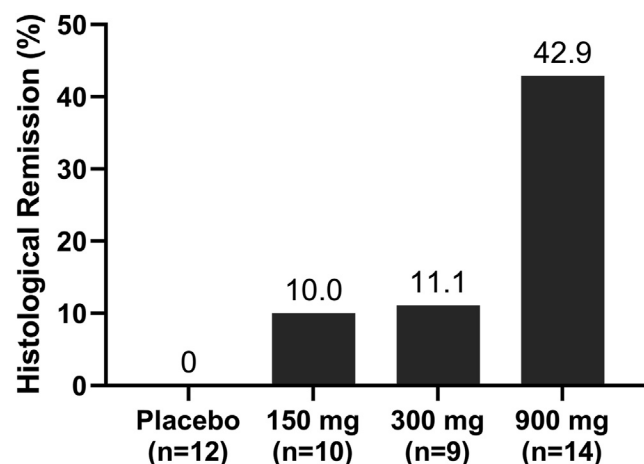


Figure 2. Dose-dependent evidence of histologic remission by PTG-100. Histologic remission was defined as a week 12 Robarts Histopathologic Index score of ≤ 3 (with an absence of neutrophils and no erosions or ulcerations) among participants who had a score of >3 at baseline.

900-mg dose vs 0 of 13 (0%) for placebo.²² Histologic remission as indicated by a Geboes score of <2.0 was 0 of 15 (0%) in placebo group and 2 of 15 (13.3%) at the 900-mg dose. Minimal histologic disease activity or histologic improvement as indicated by a Geboes score of <3.2 occurred in 3 of 15 (20%) in the placebo group and 7 of 15 (46.7%) at the 900-mg dose among paired samples. Together, these data suggest that PTG-100 improves histologic disease.

To determine if PTG-100 localizes to colonic tissues, we performed immunohistochemistry of colon biopsy samples from 10 patients of the 900-mg cohort using an anti-PTG-100 antibody as the detection reagent. Digital image analysis of slides at screening and week 12 indicated specific staining of PTG-100 within the lamina propria and lymphoid aggregates of all patients analyzed (Figure 3). In conclusion, these data confirm that PTG-100 localizes to the lamina propria and lymphoid aggregates of colonic epithelial cells in patients with UC.

Phase 2a safety. In this phase 2a study, PTG-100 was well tolerated. Adverse events were infrequent and mostly mild. No serious infections were reported, and SAEs were all related to underlying UC complications or worsening symptoms of UC. In total, 6 participants had SAEs (5 active PTG-100 and 1 placebo). No serious GI infections, included but not limited to abscesses, de novo *C difficile* infections, or reactivation of cytomegalovirus colitis, were observed. No cases of progressive multifocal leukoencephalopathy were reported. There was 1 SAE in the placebo group that led to

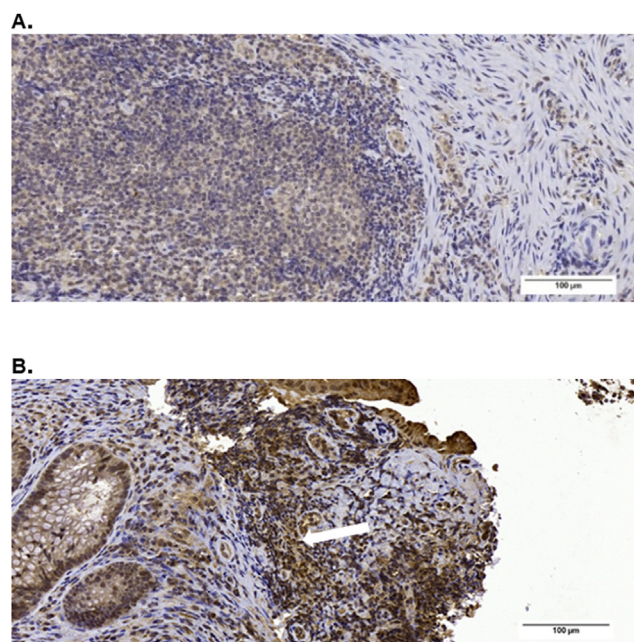


Figure 3. Immunohistochemistry staining of PTG-100 within colon biopsy samples from the same 900-mg dose cohort patient at (A) screening and (B) day 84. The arrow indicates localized staining within the lymphoid follicle region. Image analysis indicated that staining was specific because the percentage of PTG-100-positive cells stained by the antibody was higher compared to samples stained in the presence of antibody and an excess of PTG-100 blocking peptide.

death reported in the study. The participant was a 57-year-old White man diagnosed with GI disorders, intestinal ischemia, and mesenteric ischemia of the small intestine. The SAE lasted 36 days; was considered severe, not related to the study drug; and required hospitalization, and the outcome was fatal.

Phase 2a study pharmacokinetics/pharmacodynamics. In support of the overall safety and tolerability seen in this phase 2a study, pharmacokinetic analyses from all participants who received PTG-100 showed low systemic exposure after once-daily dosing up to 900 mg for 12 weeks. The overall plasma concentrations of PTG-100 detected ranged from 0–143 ng/mL. Plasma exposure of PTG-100 showed a dose-dependent increase. In participants receiving 150 mg, 300 mg, or 900 mg of PTG-100, the mean C_{max} values on day 0 were 1.3, 2.7, and 5.5 ng/mL, respectively, and the mean area under the plasma concentration curve to the last sampling point (AUC_{0-t}) values were 2.9, 5.9, and 9.7 ng·h/mL, respectively; on day 84, the mean C_{max} values were 1.7, 4.7, and 15.0 ng/mL, respectively, and the mean AUC_{0-t} values were 5.7, 11.4, and 38.3 ng·h/mL, respectively. PD analyses, including RO and decreases in RE in circulating $\alpha 4\beta 7$ lymphocyte populations, confirmed the target engagement of PTG-100. The mean RO values in T memory cells at 4 hours postdose (close to T_{max}) in the 150-mg, 300-mg, and the 900-mg dose cohorts on day 0 were 18.1%, 30.1%, and 51.2%, respectively, and after the 12-week dosing period, trough RO values were 6.6%, 33.4%, and 63.5%, respectively. Corresponding PTG-100 trough concentrations were 0.5, 3.8, and 7.1 ng/mL. Figure 4 shows the trough PD responses for RO and RE from day 14 to day 84. The data show that PTG-100 dosing caused a sustained PD effect throughout the 12-week trial and indicate that

PTG-100 does not require 100% RO to achieve measurable clinical remission.

PTG-100's effects on lymphocyte cell trafficking were shown by a significant increase in the percentage of circulating CD4⁺ memory $\alpha E^{-}\alpha 4^{+}\beta 7^{+}$ T cells compared to placebo after 12 weeks of dosing (Supplementary Figure 10). This increase was specific to the gut-homing $\beta 7^{+}$ T cells because no significant increase was observed for the $\alpha E^{-}\alpha 4^{+}\beta 7^{-}$ T cells. There were also significant increases in circulating blood gut-homing B cells (CD45⁺CD3⁺CD19⁺IgD⁺ $\alpha 4^{+}\beta 7^{+}$) compared to placebo (data not shown).

Discussion

New safe and effective oral treatments are needed for patients with moderate to severe IBD. The JAK inhibitor tofacitinib is approved for the treatment of moderate to severe UC, but its use may be limited by safety risks, including serious infection and thromboembolic events. Ozanimod, an agonist of the sphingosine-1-phosphate (S1P) receptor, was also recently approved for UC. PTG-100 is an orally administered peptide antagonist of the $\alpha 4\beta 7$ receptor expressed on the surface of lymphocytes. Potential advantages of an $\alpha 4\beta 7$ antagonist with high gut exposure include the potential for increased efficacy while maintaining an excellent safety profile, which has been reported with systemic monoclonal antibody therapy with the $\alpha 4\beta 7$ antagonist vedolizumab. A safe, well-tolerated, and effective oral treatment may be ideal for patients who prefer to avoid injections. Furthermore, the option of a GI-specific mechanism may be suitable for younger patients who are naive to biologic and other advanced therapies, thus allowing broadly systemic immunosuppressive agents to be used at later stages of UC treatment.

PTG-100 has limited systemic exposure, and preclinical studies showed higher levels of target engagement in the GALT compared to blood at doses that affect trafficking within the blood compartment. In this phase 2a study, the 900-mg dose cohort demonstrated penetration into local tissues, showing accumulation of PTG-100 within the lamina propria and lymphoid aggregates of colon biopsy samples. Dose-dependent evidence of histologic remission was clearly observed among patients who received PTG-100 compared to placebo, consistent with the therapeutic effect attributable to penetration of PTG-100 into the submucosal GI tissues. Clinical remission was also clearly evident in participants who received 900 mg of PTG-100. Together, these data support evidence that clinical efficacy for an oral $\alpha 4\beta 7$ integrin antagonist does not require full target saturation in the peripheral blood.

PTG-100 given in single and multiple ascending doses in healthy participants resulted in a minimal and dose-dependent increase in systemic exposure. The low systemic exposure is not surprising given that large molecular weight, hydrophobicity, and low intrinsic intestinal permeability contribute to the poor systemic absorption of most peptides administered orally. Notably, very little intact PTG-100 was recovered in the urine. Fecal recovery of intact

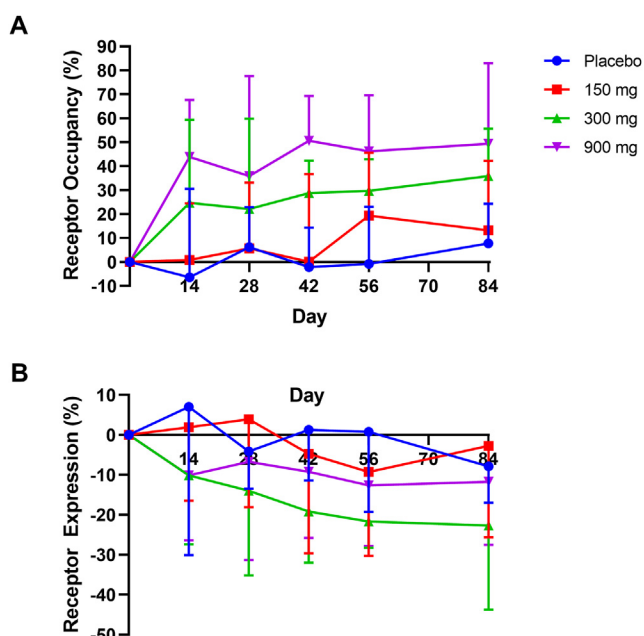


Figure 4. PD responses of PTG-100 in participants with UC as measured by (A) percent RO or (B) percent RE of circulating $\alpha 4\beta 7^{+}$ CD4⁺ T memory lymphocytes.

PTG-100 was modest and dose dependent, ranging from 7.6% to 15.8% at 300 mg and 1000 mg, respectively. Although in vitro studies demonstrate the stability of PTG-100 in GI fluids and intestinal S9 fractions, PTG-100 metabolism is noted in the presence of pancreatic enzymes. This may, in part, explain the lower fecal recovery in the clinical study. Therefore, although some fraction of PTG-100 remained stable enough to be recovered in the feces, the majority of the drug may have been degraded in the GI lumen. The low systemic and high gut exposure of PTG-100 is consistent with it being well tolerated in participants.

Overall, these results support the hypothesis that preclinical and clinical efficacy by an oral $\alpha 4\beta 7$ integrin antagonist does not require full target engagement (100% RO) in the peripheral blood. Blood RO levels achieved were consistent with those observed in healthy participants and in preclinical studies showing preclinical efficacy at blood RO levels markedly less than 100%. In the phase 2a trial in participants with UC, improvements in clinical remission and endoscopic responses were also associated with blood RO levels of <100% and similar to those observed in the phase 1 and preclinical studies. Despite blood RO being <100%, PTG-100 900 mg affected trafficking of blood gut-homing T cells as measured by increases in circulating cell percentages, similar to the effects observed in preclinical studies (and similar to what has been reported with vedolizumab). Together, these findings suggest that PTG-100 (and perhaps vedolizumab) may also act by mechanisms distinct from T-cell homing, that is, by affecting cell-cell interactions in already trafficked cells.

The prevailing mechanism by which vedolizumab is thought to reduce GI inflammation in patients with IBD is by only decreasing trafficking of circulatory T cells into the intestinal mucosa, but there are insufficient clinical data to support this.²³ The vedolizumab serum trough concentrations required for clinical efficacy are more than 16-fold those needed for complete $\alpha 4\beta 7$ integrin saturation in blood, suggesting that a concentration gradient may be required for the antibody to reach the local extravascular GI tissue to be clinically effective. Further support for a mechanism of action distinct from T-cell homing comes from PN-943, a second-generation analog of PTG-100, which has shown superior preclinical properties and improved levels of target engagement in healthy volunteers because of its greater potency.^{24,25} In preclinical studies, PN-943 was also shown to inhibit MAdCAM-1-dependent proliferation and release of proinflammatory cytokines from CD4⁺ T-cells in a concentration-dependent manner.²⁶ These observations are consistent with local mechanism(s) independent of effects on trafficking for an $\alpha 4\beta 7$ integrin antagonist.

In summary, although this phase 2 study initially did not meet the primary endpoint, PTG-100 showed proof-of-concept efficacy in patients with moderate to severe active UC. This was shown by dose-dependent increases in clinical remission, endoscopic improvement, and histologic remission in PTG-100 recipients versus those receiving placebo. The data support the therapeutic potential of an oral peptide antagonist of $\alpha 4\beta 7$ with limited systemic exposure among patients with UC.

Supplementary Material

Note: To access the supplementary material accompanying this article, visit the online version of *Gastroenterology* at www.gastrojournal.org, and at <https://doi.org/10.1053/j.gastro.2021.08.045>.

References

1. Picarella D, Hurlbut P, Rottman J. Monoclonal antibodies specific for β_7 integrin and mucosal addressin cell adhesion molecule-1 (MAdCAM-1) reduce inflammation in the colon of *scid* mice reconstituted with DC45RB^{high} CD4⁺ T cells. *J Immunol* 1997;158:2099–2106.
2. Hesterberg P, Winsor-Hines D, Briskin J, et al. Rapid resolution of chronic colitis in the cotton-top tamarin with an antibody gut-homing integrin $\alpha 4\beta 7$. *Gastroenterology* 1996;111:1373–1380.
3. Neurath M. Current and emerging therapeutic targets for IBD. *Nat Rev Gastroenterol Hepatol* 2017;14:269–278.
4. Feagan BG, Rutgeerts P, Sands BE, et al. Vedolizumab as induction and maintenance therapy for ulcerative colitis. *N Engl J Med* 2013;369:699–710.
5. Sandborn W, Feagan BG, Rutgeerts P, et al. Vedolizumab as induction and maintenance therapy for Crohn's disease. *N Engl J Med* 2013;369:711–721.
6. Zundler S, Becker E, Schulze LL, et al. Immune cell trafficking and retention in inflammatory bowel disease: mechanistic insights and therapeutic advances. *Gut* 2019;68:1688–1700.
7. Rosario M, French J, Dirks N, et al. Exposure–efficacy relationships for vedolizumab induction therapy in patients with ulcerative colitis or Crohn's disease. *J Crohns Colitis* 2017;11:921–929.
8. Rosario M, Dirks N, Milch C, et al. A review of the clinical pharmacokinetics, pharmacodynamics, and immunogenicity of vedolizumab. *Clin Pharmacokinet* 2017;56:1287–1301.
9. Ungar B, Kopylov U, Yavzori M, et al. Association of vedolizumab level, anti-drug antibodies, and $\alpha 4\beta 7$ occupancy with response in patient with inflammatory bowel disease. *Clin Gastroenterol Hepatol* 2018;16:697–705.
10. Schulze H, Esters PHartmann F, et al. A prospective cohort study to assess the relevance of vedolizumab drug levels in monitoring in IBD patients. *Scand J Gastroenterol* 2018;53:670–676.
11. US Department of Health and Human Services, Food and Drug Administration, Center for Drug Evaluation and Research. Ulcerative colitis: clinical trial endpoints. Guidance for industry. August 2016. Available at: <https://www.fda.gov/media/99526/download>. Accessed September 28, 2021.
12. Yaras A, Maher S, Bayless M, et al. The Inflammatory Bowel Disease Questionnaire in randomized controlled trials of treatment for ulcerative colitis: systematic review and meta-analysis. *J Patient Cent Res Rev* 2020;7:189–205.
13. Pai RK, Jairath V, Castele NV, et al. The emerging role of histologic disease activity assessment in ulcerative colitis. *Gastrointest Endosc* 2018;88:887–898.

14. Yu Y, Zhu Jiangai, Mi L-Z, et al. Structural specializations of $\alpha_4\beta_7$, an integrin that mediates rolling adhesion. *J Cell Biol* 2012;196:131–146.
15. Iwata M, Hirakiyama A, Eshima Y, et al. Retinoic acid imprints gut-homing specificity on T cells. *Immunity* 2004;21:527–538.
16. Soler D, Chapman T, Wyant T, et al. The binding specificity and selective antagonism of vedolizumab, an anti- $\alpha_4\beta_7$ integrin therapeutic antibody in development for inflammatory bowel disease. *J Pharmacol Exp Ther* 2009;330:864–875.
17. Holm TL, Poulsen SS, Markholst H, Reedtz-Runge S. Pharmacological evaluation of SCID T cell transfer model of colitis: as a model of Crohn's disease. *Int J Inflam* 2012;2012:412178.
18. Vermeire S, Sandborn WJ, Danese S, et al. Anti-MAdCAM antibody (PF-00547659) for ulcerative colitis (TUR-ANDOT): a phase 2, randomised, double-blind, placebo-controlled trial. *Lancet* 2017;390(10090):135–144.
19. Sandborn WJ, Su C, Sands BE, et al. OCTAVE induction 1, OCTAVE induction 2, and OCTAVE sustain investigators. Tofacitinib as induction and maintenance therapy for ulcerative colitis. *N Engl J Med* 2017;376:1723–1736.
20. Sandborn WJ, Feagan BG, Wolf DC, et al. Ozanimod induction and maintenance treatment for ulcerative colitis. *N Engl J Med* 2016;374:1754–1762.
21. Vermeire S, O'Byrne S, Keir M, et al. Etrolizumab as induction therapy for ulcerative colitis: a randomized, controlled, phase 2 trial. *Lancet* 2014;384:309–318.
22. Sandborn WJ, Bressler B, Lee S, et al. PTG-100, an oral gut-restricted peptide antagonist, induces clinical and histologic remission in patients with moderate to severely active ulcerative colitis. *United European Gastroenterol J* 2018;6:1586–1587.
23. Rogler G. Mechanism of action of vedolizumab: do we really understand it? *Gut* 2019;68:4–5.
24. Mattheakis L, Tang T, Venkataraman S, et al. The oral $\alpha_4\beta_7$ integrin specific antagonist PN-10943 is more effective than PTG-100 in multiple preclinical studies. *Gastroenterology* 2019;156(Suppl 6):S80–S81.
25. Gupta SK, Cheng X, Kanwar B, et al. Safety, pharmacokinetics, and pharmacodynamics of the novel oral peptide therapeutic PN-10943 in normal healthy volunteers. *Am J Gastroenterol* 2019;114:S430–S431.
26. Cheng L, Venkataraman S, Zhao L, et al. PN-943, an oral $\alpha_4\beta_7$ integrin antagonist, inhibits MAdCAM1-mediated proliferation and cytokine release from CD4+ T-cells independent of trafficking. Paper presented at: 15th Congress of European Crohn's and Colitis Organisation; February 15, 2020; Vienna, Austria.

CRediT Authorship Contributions

William J. Sandborn, MD (Conceptualization: Lead; Data curation: Lead; Formal analysis: Lead; Investigation: Lead; Methodology: Lead; Supervision: Lead; Writing – original draft: Lead; Writing – review & editing: Lead); Larry C. Mattheakis, PhD (Data curation: Supporting; Formal analysis: Supporting; Investigation: Supporting; Methodology: Supporting; Project administration: Supporting; Supervision: Supporting; Writing – original draft: Supporting; Writing – review & editing: Supporting); Nishit B. Modi, PhD (Data curation: Supporting; Formal analysis: Supporting; Writing – original draft: Supporting; Writing – review & editing: Equal); David Pugatch, MD (Data curation: Supporting; Formal analysis: Supporting; Project administration: Supporting; Writing – original draft: Supporting; Writing – review & editing: Supporting); Brian Bressler, MD, MS, FRCPC (Investigation: Equal; Writing – review & editing: Supporting); Scott Lee, MD (Investigation: Equal; Writing – review & editing: Supporting); Raj Bhandari, MD (Investigation: Equal; Writing – review & editing: Supporting); Bittoo Kanwar, MD (Conceptualization: Supporting; Data curation: Supporting; Formal analysis: Supporting; Methodology: Supporting; Project administration: Supporting; Writing – original draft: Supporting; Writing – review & editing: Supporting); Richard Shames, MD (Conceptualization: Supporting; Data curation: Supporting; Formal analysis: Supporting; Methodology: Supporting; Writing – original draft: Supporting; Writing – review & editing: Supporting); Geert D'Haens, MD, PhD (Conceptualization: Equal; Investigation: Equal; Writing – review & editing: Supporting); Stefan Schreiber, MD, PhD (Conceptualization: Equal; Investigation: Equal; Writing – review & editing: Supporting); Silvio Danese, MD, PhD (Investigation: Supporting; Writing – review & editing: Supporting); Brian Feagan, MD (Conceptualization: Equal; Investigation: Equal; Writing – review & editing: Supporting); Rish K. Pai, MD, PhD (Formal analysis: Supporting; Methodology: Supporting; Writing – review & editing: Supporting); David Y. Liu, PhD (Data curation: Supporting; Formal analysis: Supporting; Project administration: Supporting; Resources: Supporting; Supervision: Supporting; Writing – original draft: Supporting; Writing – review & editing: Supporting); Suneel Gupta, PhD (Data curation: Supporting; Formal analysis: Supporting; Project administration: Supporting; Resources: Supporting; Supervision: Supporting; Writing – original draft: Equal; Writing – review & editing: Supporting).

Conflicts of interest

William Sandborn has received research grants from AbbVie, Abivax, Arena Pharmaceuticals, Boehringer Ingelheim, Celgene, Genentech, Gilead Sciences, GlaxoSmithKline, Janssen, Lilly, Pfizer, Prometheus Biosciences, Seres Therapeutics, Shire, Takeda, Theravance Biopharma; has received consulting fees from AbbVie, Abivax, Admrx, Alfasigma, Alimentiv (previously Robarts Clinical Trials, owned by Alimentiv Health Trust), Alivio Therapeutics, Allakos, Amgen, Applied Molecular Transport, Arena Pharmaceuticals, Bausch Health (Salix), Beigene, Bellatrix Pharmaceuticals, Boehringer Ingelheim, Boston Pharmaceuticals, Bristol Myers Squibb, Celgene, Celltrion, Cellularity, Cosmo Pharmaceuticals, Escalier Biosciences, Equillum, Forbion, Genentech/Roche, Gilead Sciences, Glenmark Pharmaceuticals, Gossamer Bio, Immuniv (Vital Therapies), Index Pharmaceuticals, Intact Therapeutics, Janssen, Kyverna Therapeutics, Landos Biopharma, Lilly, Oppilan Pharma, Otsuka, Pandion Therapeutics, Pfizer, Progenity, Prometheus Biosciences, Protagonists Therapeutics, Provention Bio, Reistone Biopharma, Seres Therapeutics, Shanghai Pharma Biotherapeutics, Shire, Shoreline Biosciences, Sublimity Therapeutics, Surrozen, Takeda, Theravance Biopharma, Thetis Pharmaceuticals, Tillotts Pharma, UCB, Vendata Biosciences, Ventyx Biosciences, Vimalan Biosciences, Vivelix Pharmaceuticals, Vivreon Biosciences, and Zealand Pharma; holds stock or stock options from Allakos, BeiGene, Gossamer Bio, Oppilan Pharma, Prometheus Biosciences, Progenity, Shoreline Biosciences, Ventyx Biosciences, Vimalan Biosciences, Vivreon Biosciences; is an advisor/speaker for Ferring, Janssen, AbbVie, Takeda, Pfizer, Novartis, Bristol Myers Squibb, and Merck; is an advisor for Alimentiv, Gilead, Iterative Scopes, Applied Molecular Transport, Celgene, Microbiome Insights, Merck, Amgen, Pendopharm, Genentech, Allergan, Protagonist, Fresenius Kabi, and Mylan; has received research support from Janssen, AbbVie, GlaxoSmithKline, Bristol Myers Squibb, Amgen, Genentech, Merck, Boehringer Ingelheim, Qu Biologic, Celgene, Alvine; and has received stock options from Qu Biologic. Larry C. Mattheakis is an employee and shareholder of Protagonist Therapeutics, Inc. Nishit B. Modi is an employee and shareholder of Protagonist Therapeutics, Inc. Brian Bressler is an advisor/speaker for Ferring, Janssen, AbbVie, Takeda, Pfizer, Novartis, Bristol Myers Squibb, and Merck; is an advisor for Alimentiv, Gilead, Iterative Scopes, Applied Molecular Transport, Celgene, Microbiome Insights, Merck, Amgen, Pendopharm, Genentech, Allergan, Protagonist, Fresenius Kabi, and Mylan; has received research support from Janssen, AbbVie, GlaxoSmithKline, Bristol Myers Squibb, Amgen, Genentech, Merck, Boehringer Ingelheim, Qu Biologic, Celgene, Alvine; and has received stock options from Qu Biologic. Scott Lee has received grant/research support from AbbVie, UCB Pharma, Janssen, Salix, Takeda, Arena, and AbGenomics and has served as a consultant for UCB Cornerstone Health, Janssen, Eli Lilly, Celgene, KCRN Research, Boehringer Ingelheim, Bristol Myers Squibb, Applied Molecular Transport,

Received December 30, 2020. Accepted August 9, 2021.

Correspondence

Address correspondence to: Suneel Gupta, PhD, Protagonist Therapeutics, 7707 Gateway Boulevard, Suite 140, Newark, California 94560-1160. e-mail: s.gupta@ptgx-inc.com.

Acknowledgments

Desiree Hollemon, MSN, MPH, provided writing assistance for the manuscript that was paid for by Protagonist Therapeutics.

Arena, Celltrion, Samsung Biopis, Bridge and Biotherapeutics. Bittoo Kanwar is a former employee of Protagonist Therapeutics, Inc. Richard Shames is a former employee of Protagonist Therapeutics, Inc. Geert D'Haens has served as an advisor for AbbVie, Ablynx, Active Biotech AB, Agomab Therapeutics, Alimentiv, Allergan, Alphabionics, Amakem, Amgen, AM Pharma, Applied Molecular Therapeutics, Arena Pharmaceuticals, AstraZeneca, Avaxia, Biogen, Bristol Myers Squibb/Celgene, Boehringer Ingelheim, Celltrion, Cosmo, DSM Pharma; Echo Pharmaceuticals, Eli Lilly, Engene, Exelion Biosciences; Ferring, Dr Falk Pharma, Galapagos, Genentech/Roche, Gilead, GlaxoSmithKline, Gossamerbio, Pfizer, Immuniv, Johnson & Johnson, Kintai Therapeutics, Lument, Lycera, Medimetrics, Takeda, Medtronic, Mitsubishi Pharma, Merck Sharp Dohme, Mundipharma, Nextbiotics, Novo Nordisk, Otsuka, Photopill, ProciseDx, Prodigest, Prometheus Laboratories/Nestle, Progenity, Protagonist, RedHill, Salix, Samsung Bioepis, Sandoz, Seres/Nestec/Nestle, Setpoint, Shire, Teva, Tigenix, Tillotts, Topivert, Versant, and Vifor. Stefan Schreiber has been a consultant for AbbVie, Bristol Myers Squibb, Boehringer Ingelheim, Ferring, Genentech/Roche, Janssen, Lilly, Medimmune/AstraZeneca, Novartis, Merck Sharp Dohme, Pfizer, Protagonist, Sanofi, Takeda, Theravance, and UCB and is a paid speaker for AbbVie, Ferring, Janssen, Merck Sharp Dohme, Novartis, Takeda, and UCB. Silvio Danese has received research grants from AbbVie, Amgen, Celgene, Genentech, Gilead, Janssen, Pfizer, Receptos (Celgene), Robarts Clinical Trials, Seres Therapeutics, Takeda, and UCB and has been a consultant for AbbVie, Allergan, Amgen, Bristol Myers Squibb, Celgene, Celltrion, Janssen, Lilly, Pfizer, Takeda, and UCB. Brian Feagan has received grant/research support from AbbVie Inc, Amgen Inc, AstraZeneca/MedImmune Ltd, Atlantic Pharmaceuticals Ltd, Boehringer

Ingelheim, Celgene Corporation, Celltech, Genentech Inc/Hoffmann-La Roche Ltd, Gilead Sciences Inc, GlaxoSmithKline, Janssen Research & Development LLC, Pfizer Inc, Receptos Inc/Celgene International, Sanofi, Santarus Inc, Takeda Development Center Americas Inc, Tillotts Pharma AG, and UCB and is a consultant for Abbott/AbbVie, AgomAB Therapeutics, Allakos, Allergan, Amgen, Applied Molecular Transport, Aptevio Therapeutics, AstraZeneca, Atlantic Pharma, BioMx Israel, Boehringer Ingelheim, Bristol Myers Squibb, Calypso Biotech, Celgene, Connect BioPharma, Everest Clinical Research Corp, Galapagos, Galen Atlantica, Genentech/Roche, Gilead, Gossamer Pharma, GlaxoSmithKline, Hoffmann-LaRoche, Index Pharma, Janssen, Kaleido Biosciences, Kyowa Kakko Kirin Co Ltd, Lilly, Lument AB, Merck, Millenium, Mylan, Nestles, Nextbiotix, Origo BioPharma, Pandion Therapeutics, ParImmune, Parvus Therapeutics Inc, Pfizer, Prometheus Therapeutics and Diagnostics, Progenity, Protagonist, Qu Biologics, Rebiotix, Receptos, Salix Pharma, Sandoz, Sanofi, Shire, Surroze Inc, Takeda, Tillotts, UCB Pharma, VHSquared Ltd, Ysios, and Zealand Pharma. Rish K. Pai is a former employee of Protagonist Therapeutics, Inc, and has received consulting fees from AbbVie, Genentech, Eli Lilly, Allergan, PathAI, and Alimentiv. David Y. Liu is an employee and shareholder of Protagonist Therapeutics, Inc. Suneel Gupta is an employee and shareholder of Protagonist Therapeutics, Inc. The remaining authors disclose no conflicts.

Funding

Protagonist Therapeutics provided funding through investigator research grants for the conduct of clinical trials described in this study. The sponsor was involved in the study design, collection, analysis, interpretation of data, and preparation of the manuscript.

Supplementary Methods

Preclinical Studies

Preclinical Study Materials. PTG-100, PN10941, PN10973, and PN10967 were synthesized at Protagonist Therapeutics USA. Vedolizumab was provided by Aragen Bioscience.

Cell Adhesion Assays. For primary cell assays, leukopaks were obtained from the Stanford Blood Bank and human CD4⁺ memory T cells isolated by magnetic separation (StemCell Technologies, catalog no. 19157). Human RPMI8866 (Sigma, catalog no. 95041316), mouse TK1 (ATCC, catalog no. ATCC-CRL-2396), and human Jurkat E 6.1 cells (Sigma, catalog no. 88042803) were cultured using the supplier's recommended conditions. For CD4⁺ memory T-cell adhesion assays, capture antibody IgG Fc (AffiniPure Donkey Anti-Human IgG, Fc Fragment Specific, Jackson Immuno Research, catalog no. 709-005-098) was immobilized onto a high-binding capacity plate (FLUOTRAC 600/black, clear bottom, Greiner Bio-One, catalog no. 655077) at a concentration of 500 ng/well in 50 mmol/L sodium bicarbonate buffer, pH 9.5, and incubated overnight at 4°C. The plate was rinsed twice with Blocking Buffer (25 mmol/L Tris HCl, pH7.5; 150 mmol/L NaCl; 1.5% bovine serum albumin [BSA]; 0.05% Tween). Human MAdCAM-1 (R&D Systems, catalog no. 6056-MC), VCAM-1 (R&D Systems, catalog no. 862-VC), or ICAM-1 (R&D Systems, catalog no. 720-IC) were added at 400 ng/well in blocking buffer, and the plate was incubated overnight at 4°C. For the RPMI8866, TK1, and Jurkat cell assays, human MAdCAM-1 or VCAM-1 was coated directly onto Nunc MaxiSorp plate (Thermo Scientific, catalog no. 439454) at 200 ng/well and incubated overnight at 4°C, followed by a 1-hour incubation at 37°C in blocking buffer. Cells were resuspended in binding buffer (Dulbecco's modified Eagle medium phenol red-free, 10 mmol/L HEPES, 1× Na pyruvate, 1× glutamine, 1 mmol/L MnCl₂) and plated at 700,000 cells/well CD4⁺ memory T cells or 200,000 cells/well for RPMI8866, TK1, and Jurkat. Plates were incubated at 37°C, 5% CO₂ for 0.75–1.5 hours to allow for cell adhesion. Unbound cells were removed by washing 3 times with binding buffer, and the remaining bound cells were counted using CyQUANT (Invitrogen Life Technologies, catalog no. C35006) for primary cells or (3-(4,5-dimethylthiazol-2-yl)-2,5-diphenyltetrazolium bromide (MTT) cell proliferation (ATCC, catalog no. 30-1010K) for RPMI8866, TK1, and Jurkat. IC₅₀ values were calculated using 4-parameter nonlinear fit of the data.

Surface Plasmon Resonance Binding. Binding studies were performed at 25°C using a Biacore T100 optical biosensor equipped with a streptavidin-coated sensor chip and equilibrated with running buffer (50 mmol/L Tris-HCl, 150 mmol/L NaCl, 0.5% BSA, 0.05% Tween-20, 1 mmol/L MnCl₂, pH 7.5). Five hundred micrograms of $\alpha 4\beta 7$ integrin protein (R&D Systems, catalog no. 5397-A3, lot SEY2014031) was dissolved into running buffer to yield a stock concentration of 880 nmol/L. Biotinylated PTG-100 (PN-10941) or vedolizumab was captured on the sensor chip to densities of 140–550 resonance units. The integrin

was tested for binding to the streptavidin-captured targets using 880 nmol/L as the highest concentration in 3-fold dilution series. Each concentration of the integrin was injected for 1 hour, and then its dissociation from the surfaces was monitored for another hour. The target surfaces were regenerated with a 10-second injection of 120 mmol/L HCl at the end of each binding cycle. For kinetic analyses of integrin/target interactions, each data set was globally fit to a 1:1 interaction model to obtain the listed binding parameters.

Schild Analysis of Binding by Enzyme-Linked Immunosorbent Assay. Recombinant human integrin $\alpha 4\beta 7$ (R&D Systems, catalog no. 5397-A30) was coated onto a nickel-coated plate (Pierce, catalog no. 15442) at a concentration of 800 ng/well. Wells were blocked and washed, and dilutions of human MAdCAM-1 Fc chimera protein (R&D Systems, catalog no. 6056-MC-050) were added in the presence of different fixed concentrations of PTG-100 at 0, 1, 3, 10, and 30 nmol/L. After a 2-hour incubation at room temperature, detection was performed by mouse anti-human IgG1-HRP (Invitrogen, catalog no. A10648). Schild analysis was by the Gaddum/Schild EC₅₀ shift equation in GraphPad software Prism 7 (GraphPad Software, Inc).

In Vitro Binding of PTG-100 to Activated Peripheral Blood Mononuclear Cells. Human PBMCs were cultured for 7 days in the absence (control) or presence of anti-CD3 (5 μ g/mL), human interleukin 2 (20 ng/mL), or retinoic acid (1 μ mol/L). One million cells per well were seeded before binding with 1 nmol/L Alexa Fluor 647–tagged PTG-100 (PN-10967) for 2 hours at 37°C. A portion of the control PBMCs were incubated for 15 minutes with MnCl₂ (1 mmol/L) before the addition of the peptide. Samples were stained with the following antibodies: CD45-V500, CD4-Alexa Fluor 700, CD45RA–fluorescein isothiocyanate [FITC], and vedolizumab-biotin. Samples were washed, followed by staining with streptavidin-BV421. All stained samples were analyzed by flow cytometry.

PTG-100 Binding in Human Whole Blood. Human whole blood from donors (Stanford Blood Bank) was collected using BD Vacutainer sodium heparin blood collection tubes. Manganese chloride (1 mmol/L final concentration) was added, and the samples were incubated at room temperature for 10–15 minutes. Samples were stained with the following antibodies: CD45 V500 (no. 560777) and CD19 PE-CF594 (no. 562321) from BD Biosciences and CD3 PE-Cy7 (no. 300419), CD4 Ax700 (no. 300526), CD45RA PerCP-Cy5.5 (no. 304122), CD16 Pacific Blue (no. 302032), CD56 Pacific Blue (no. 318326), and CD14 PE (no. 325606) from BioLegend. Vedolizumab-biotin or PTG-100 Ax647 was added to a final concentration of 1 nmol/L. Samples were also stained with streptavidin Ax647. Samples were analyzed using a BD LSRII flow cytometer, and singlet leukocytes were identified based on CD45 expression as well as forward scatter (FSC) and side scatter (SSC) area and width characteristics. The following gating strategy was used to define leukocyte subsets: naive CD4 T cells: CD45⁺CD3⁺CD4⁺CD45RA⁺; memory CD4 T cells: CD45⁺CD3⁺CD4⁺CD45RA⁺; naive CD8 T cells: CD45⁺CD3⁺CD8⁺CD45RA⁺; memory CD8 T cells:

CD45⁺CD3⁺CD8⁺CD45RA⁻; B cells: CD45⁺CD19⁺; natural killer cells: CD45⁺SSC^{low}CD16/CD56⁺; monocytes: CD45⁺CD14⁺; neutrophils: CD45⁺SSC^{high}CD16⁺; eosinophils: CD45⁺SSC^{high}CD16⁻; and basophils: CD45^{low}SSC^{low}CD14⁻CD3⁻CD19⁻CD16/CD56⁻. Binding of vedolizumab-biotin or PTG-100 Ax647 was quantified based on the percentage Ax647 positive, with gates set based on fluorescence minus 1 (PTG-100 Ax647) or secondary reagent (streptavidin Ax647) staining controls.

To measure the internalization of $\beta 7$ integrin, blood samples were plated into 96-well plates (0.2 mL/well) and incubated with PTG-100 (5 nmol/L), PN10973 (5 or 50 nmol/L), or dimethyl sulfoxide vehicle control. PN10973 is an inactive analog of PTG-100 containing 3 mutations. Plates were sealed with aluminum plate seals and either refrigerated at 4°C or incubated on a 37°C heat block equipped with a 96-well plate block for 1, 6, or 24 hours. Samples were stained for $\beta 7$ surface expression using a phycoerythrin (PE)-conjugated antibody (clone FIB504, BioLegend). Additional antibodies were included to allow identification of relevant leukocyte subsets: CD45 BD Horizon V500 (clone HI30) and CD19 BD Horizon PE-CF594 (clone HIB19) from BD Biosciences; CD3 antigen-presenting cell (APC) (clone UCHT1), CD4 Alexa Fluor 700 (clone RPA-T4), CD45RA FITC (clone HI100), and integrin $\alpha 4$ biotin (clone 9F10) from BioLegend; and integrin αE PE-Cy7 (clone B-Ly7) from eBioscience. Surface marker stains were performed in whole blood at 4°C for 30 minutes. After staining and fixation, samples were stained with streptavidin Brilliant Violet 421 (BioLegend) for 30 minutes at 4°C, washed, and resuspended in phosphate-buffered saline/BSA for flow cytometry analysis. Memory CD4 T cells were identified as CD45⁺, CD3⁺, CD4⁺, or CD45RA⁻ singlet lymphocytes. Memory CD4 T-cell subsets expressing vs lacking surface $\alpha E\beta 7$ integrin were identified based on staining with the anti- αE antibody. The surface expression level of integrin $\beta 7$ was evaluated for total, $\alpha E\beta 7^{+}$, and $\alpha E\beta 7^{-}$ memory CD4 T cells based on the percentage of cells showing detectable staining with the anti- $\beta 7$ PE antibody.

Immunohistochemistry of $\beta 7$ -Positive Cells in Mouse Distal Colon. Distal colon specimens were fixed in buffered 10% formalin for 24 hours and stored in 70% alcohol. The specimens were trimmed and embedded in paraffin. Formalin-fixed paraffin-embedded blocks were sectioned at 4- μ m thickness for slides and stained using ITGB7 (catalog no. 557497, rat monoclonal clone M293, BD Pharmingen) at 1 μ g/mL for 1 hour at room temperature, followed by unconjugated rabbit anti-rat secondary antibody and horseradish peroxidase-conjugated polymer reagent for 30 minutes at room temperature. Scoring was defined as the number of positive cells (reactive granulocytes) observed within a 1-mm radius of colon affected by the disease (mucosal inflammation or atrophy).

PTG-100 Stability in Gastrointestinal Fluids and Mucosal Scrapings. The in vitro stability of PTG-100 was investigated in GI fluids or mucosal scrapings of rats and pigs as well as in human intestinal fluid. In addition, estimations of PTG-100 stability in rat plasma, rat liver S9 fraction, and human intestinal S9 fraction were also

evaluated. For each evaluation, a 20- μ mol/L solution of PTG-100 was incubated at 37°C with the test system. Samples were collected, and the percentage of intact PTG-100 was measured using a liquid chromatography/tandem mass spectrometry method. The biological matrices were evaluated, and the percentage of intact PTG-100 remaining at the last incubation time point was measured. Degradation of PTG-100 was also measured using composite GI fluid from 3 human cadaver donors after a 24-hour incubation. Rat (liver) tissue 9000g supernatant (S9) was obtained from XenoTech LLC. Rat (Sprague Dawley) plasma was obtained from Pel-Freez. Porcine pancreatin and pepsin were obtained from Sigma-Aldrich. Human simulated gastric and intestinal fluid buffers were obtained from Ricca Chemical Company. Rat intestinal or colonic mucosa was prepared by homogenization of scrapings from excised tissue sections. Rat intestinal fluid was prepared by flushing the first 20 cm of excised rat small intestine or colon with 1 \times phosphate-buffered saline at pH 7.4. Human intestinal fluid (obtained from BioreclamationIVT) consisted of composite GI fluid pooled from 3 cadaver donors. The human intestinal S9 fraction and cofactors were obtained from XenoTech LLC and Sigma-Aldrich, respectively.

Mouse Flow Cytometry for Pharmacodynamics and T-Cell Trafficking Analyses. To evaluate RO in mouse samples, MnCl₂ was added to whole blood or Peyer's patch samples to a final concentration of 1 mmol/L, followed by incubation in the presence or absence of 1 μ mol/L PTG-100 to fully block the $\alpha 4\beta 7$ receptor. Blocked and unblocked samples were stained with 1 nmol/L PTG-100 Ax647, followed by staining with the following antibodies: CD45 (V500, BD Biosciences no. 561487), CD4 (Ax700, BioLegend no. 100536), B220 (PE-Cy7, BioLegend no. 103221), B220 (PerCP-Cy5.5 BioLegend no. 103235), CD44 (PE, BioLegend no. 103007), CD44 (BV421, BioLegend no. 103039), CD62L (Ax488, BioLegend no. 104419), integrin $\alpha 4$ (PE, BioLegend no. 103706), integrin $\beta 7$ (APC, BioLegend no. 321208), and integrin αE (CD103) (PE-Cy7, BioLegend no. 121426). Lymphocytes were defined by forward scatter area (FSC-A) and side scatter area (SSC-A) scatterplots, and the singlet cell population was gated by forward scatter width (FSC-W) and side scatter width (SSC-W) plots. The following gating strategy was used for T memory cells: CD45⁺CD4⁺CD44⁺CD62L⁻. To calculate the percentage of RO, blocked RO stain was used to determine the percentage of positive PTG-100 Ax647 population using the following formula:

$$[1 - (\% \text{ positive test sample} / \% \text{ positive median vehicle control})] \times 100.$$

In control studies, the percentage of RO was similar in mouse blood samples incubated in the presence or absence of 1 mmol/L MnCl₂. To assess integrin expression and cell subset abundance, whole blood samples were stained in the absence of added MnCl₂ with antibodies against $\alpha 4$, $\beta 7$, and αE , in addition to antibodies against CD45, CD4, B220, CD44, and CD62L. Samples were processed to lyse

erythrocytes and fix leukocytes, followed by wash steps. All stained samples were analyzed by flow cytometry; samples were collected as consistent volumes to permit the calculation of absolute cell counts. For T-cell trafficking studies in the mouse DSS model, the following antibodies were used: CD4 (APC, Vio770, Miltenyi no. 130-102-179), CD44 (Vio-Blue, Miltenyi no. 130-102-443), CD45RB (FITC, Miltenyi no. 130-102-461), $\alpha 4$ (APC, Miltenyi no. 130-102-142), and $\beta 7$ (PE, BD Biosciences no. 557498).

Clinical Studies

Phase 1 Study: First-in-Human Healthy Volunteers.

Participants in the phase 1 study were nonsmoking healthy men, aged 18–55 years, inclusive, with a body mass index between 18 and 30 kg/m², in generally good health, with no significant medical history and clinical laboratory parameter values within the normal range. Individuals with clinically significant abnormalities or diseases, blood pressure greater than 140/90 mm Hg, or heart rate of >100 beats per minute or clinically significant electrocardiogram abnormalities at screening were excluded.

Clinical Pharmacodynamics. For RO, blood samples were incubated with 1 mmol/L MnCl₂ and the presence or absence of 1 μ mol/L unlabeled PTG-100 to fully occupy the $\alpha 4\beta 7$ receptor. Blocked and unblocked samples were stained with 1 nmol/L PTG-100 Ax647, followed by staining with antibodies against $\alpha 4\beta 7$, CD45, CD4, CD45RA, and CD19. No MnCl₂ was added to the antibody cocktail used to evaluate integrin expression and cell subset abundance. Samples were processed to lyse erythrocytes and fix leukocytes, followed by staining with a second-step reagent (streptavidin-BV421) and wash steps. The following antibodies were used: CD45 (V500, BD Biosciences no. 560777, clone HI30), CD4 (Ax700, BioLegend no. 300526, clone RPA-T4), CD45RA (FITC, BioLegend no. 304106, clone HI100), CD19 (PE-CF594, BD Biosciences no. 562321, clone HIB19), vedolizumab-biotin (Aragen Bioscience and Protagonist), integrin $\alpha 4$ (CD49d) biotin (Primity Bio and BioLegend no. 304302, clone 9F10), integrin $\beta 7$ (PE, BioLegend no. 321204, clone FIB504), and integrin αE (CD103) (PE-Cy7, eBioscience no. 25-1038-42, clone B-Ly7). Percentage of RO was determined by median fluorescence intensity (MFI) of PTG-100 Ax647 staining subsets. The MFI values from

blocked and unblocked samples were used to calculate the extent of RO within memory CD4 T cells and memory B cells. RO was calculated according to the following formula:

$$\text{percent RO} = [1 - ([\text{unblocked}] - [\text{blocked}]) / ([\text{baseline unblocked}] - [\text{baseline blocked}])] \times 100.$$

RE was calculated as percent change of MFI from baseline for the vedolizumab stain.

Histopathology and Immunohistochemistry Colon Biopsy Preparation. Biopsy samples were immersed in 10% neutral buffered formalin and fixed overnight. Samples were transferred to 70% ethanol and shipped for processing and embedding in formalin-fixed paraffin-embedded blocks.

Supplementary Results

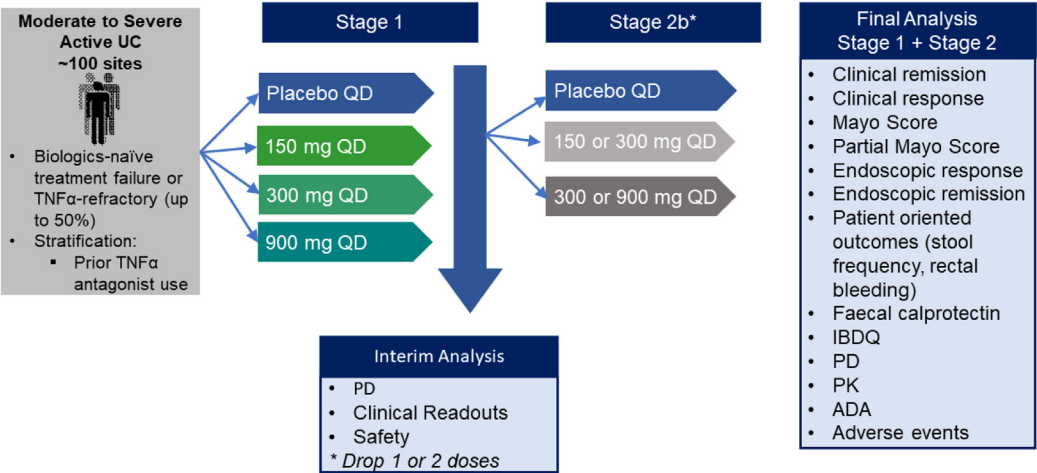
Integrin Internalization in Whole Blood

Incubation of PTG-100 in human whole blood at 37°C induced $\alpha 4\beta 7$ internalization, as measured by loss of $\beta 7$ expression on the surface of CD4⁺ memory T cells (Supplementary Figure 4). There was no substantial $\beta 7$ internalization at 37°C in vehicle-treated cells or cells treated with the mutant peptide PN10973, showing that the effect is specific for PTG-100. There was also no effect at 4°C, which confirms that binding of the anti- $\beta 7$ antibody epitope used for measuring $\beta 7$ internalization is not obscured by PTG-100 binding. Integrin internalization was detectable at as early as 1 hour on human CD4⁺ T memory cells but was most pronounced and nearly complete at 24 hours. Vedolizumab has also been reported to be internalized by $\alpha 4\beta 7$ -expressing CD4⁺ memory T cells, and the reported kinetics of internalization are similar to that of PTG-100.^{e1} The PTG-100-induced reduction in surface $\beta 7$ was also observed in naive T cells, but less so in B cells. Expression of $\alpha E\beta 7$ was not affected by PTG-100, which suggests that PTG-100 binding is specific for $\alpha 4\beta 7$, not $\alpha E\beta 7$.

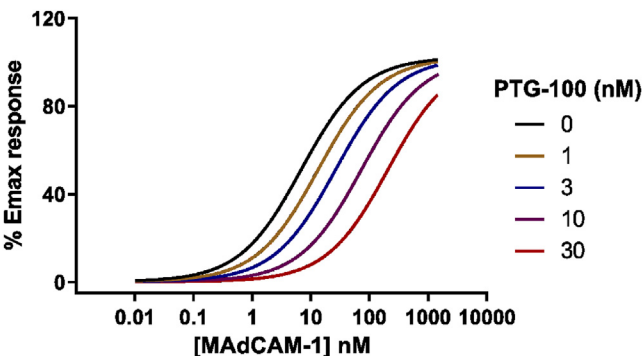
Supplementary Reference

- e1. Wyant T, Yang L, Fedyk E. In vitro assessment of the effects of vedolizumab binding on peripheral blood lymphocytes. *MAbs* 2013;5:842–850.

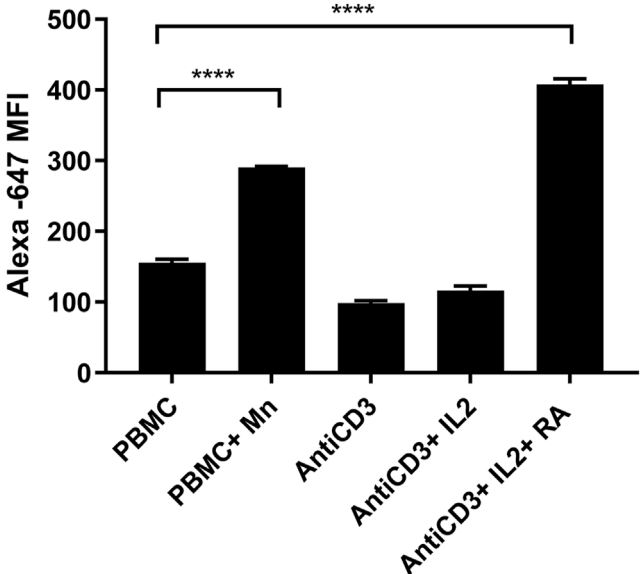
Phase 2b in UC Patients: 12 Week Induction
Randomized, Double-Blind, Placebo-Controlled Adaptive Design



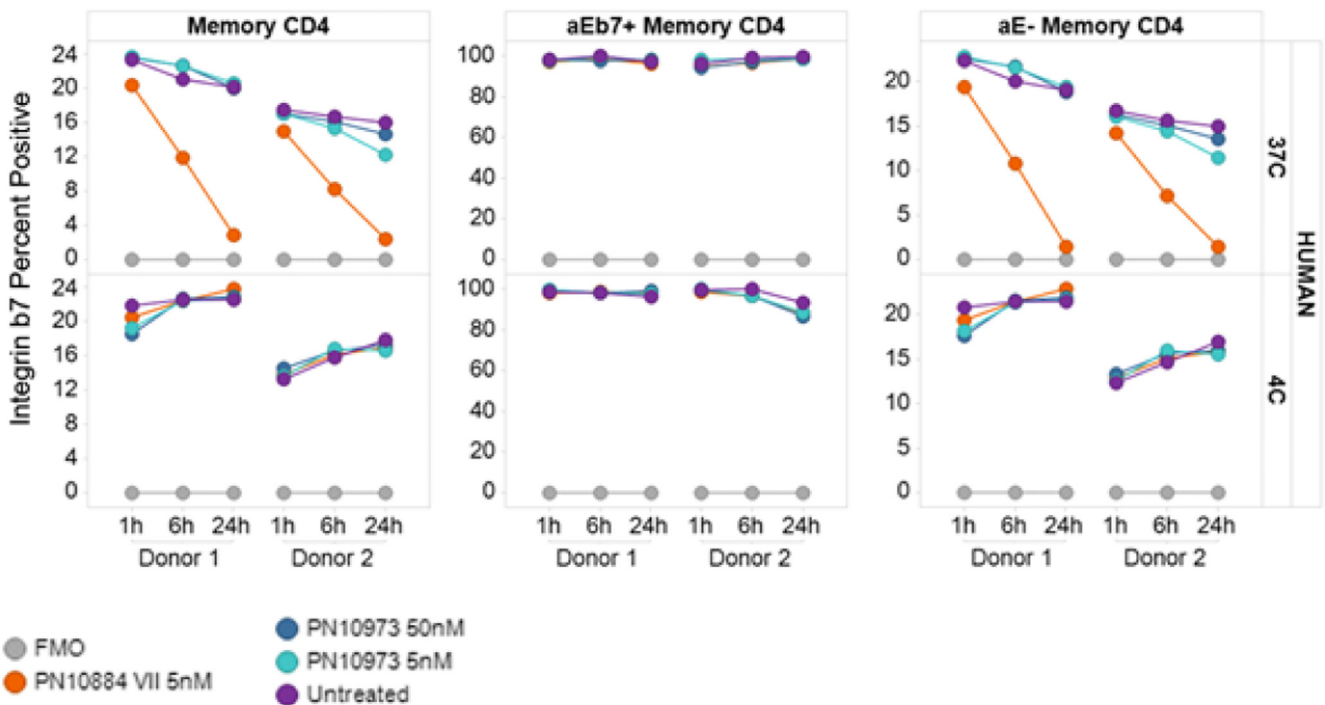
Supplementary Figure 1. Study design. ADA, antidrug antibodies; IBDQ, Inflammatory Bowel Disease Questionnaire; QD, every day; TNF, tumor necrosis factor.



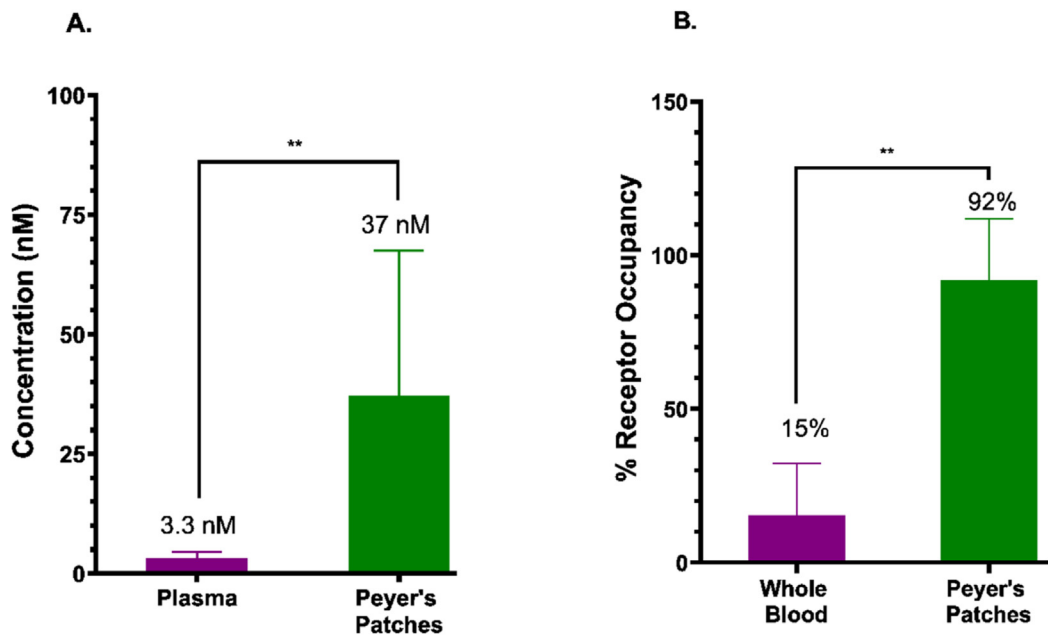
Supplementary Figure 2. Schild analysis of binding of PTG-100 to $\alpha 4\beta 7$ integrin indicates that binding is a simple reversible and competitive mechanism, as antagonism is surmountable by increasing MAdCAM-1 concentration (Schild slope, 1.008). The estimated equilibrium dissociation constant derived from the Schild analysis (K_B) value is 1 nmol/L. Emax, maximum response; M, mol/L.



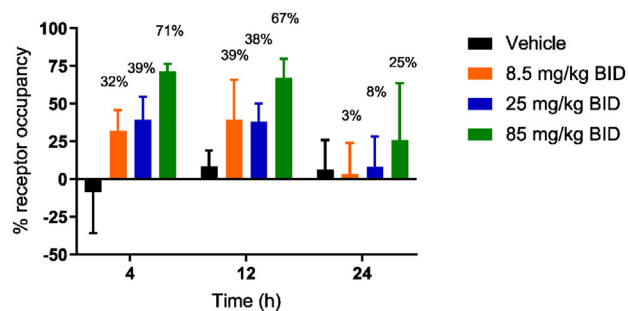
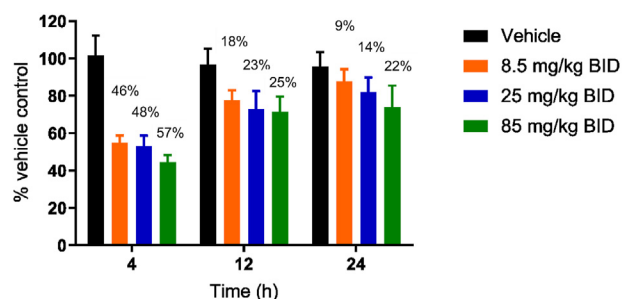
Supplementary Figure 3. Binding of Alexa Fluor 647-tagged PTG-100 (1 nmol/L) to CD4⁺CD45RA⁻ $\alpha 4\beta 7$ ⁺ memory T cells after 7-day culture under the indicated conditions. Statistical analysis was performed via 2-way analysis of variance (ANOVA) with the Dunnett multiple comparison test. *** $P < .001$; **** $P < .0001$. IL2, interleukin 2; Mn, manganese; RA, retinoic acid.



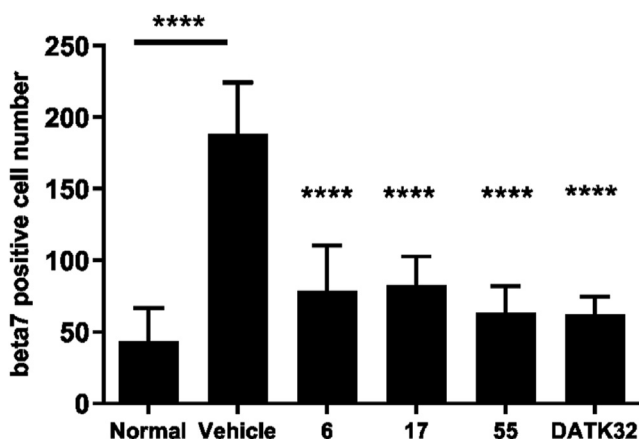
Supplementary Figure 4. PTG-100 reduces integrin $\beta 7$ surface expression on $CD4^{+}\alpha 4^{+}\beta 7^{+}\alpha E^{-}$ human memory CD4⁺ T cells, but not $CD4^{+}\alpha E^{+}\beta 7^{+}$ memory T cells. PTG-100 is also known as PN10884. FMO, fluorescence minus 1.



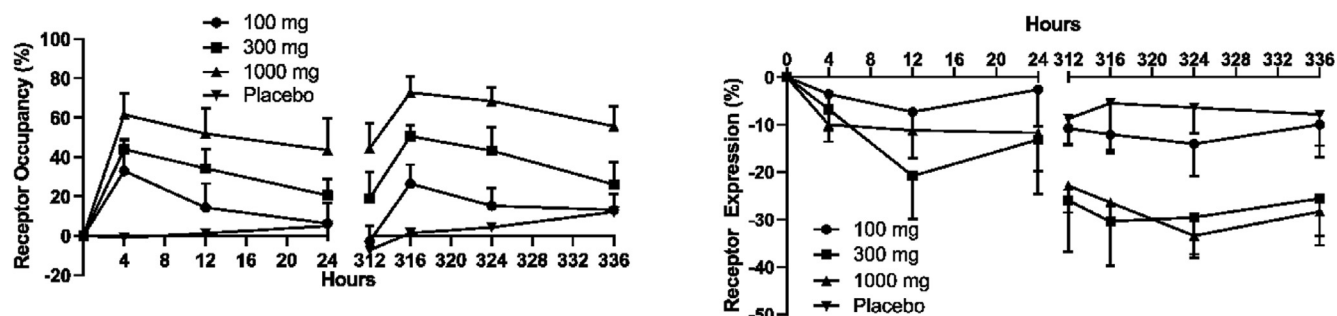
Supplementary Figure 5. Oral dosing of PTG-100 at 30 mg/kg in mice showed higher (A) exposure and (B) RO of CD4⁺ effector memory T-cells in Peyer's patches compared to whole blood. Statistical significance assessed by Mann-Whitney nonparametric test; ** $P \leq .01$.

A.**B.**

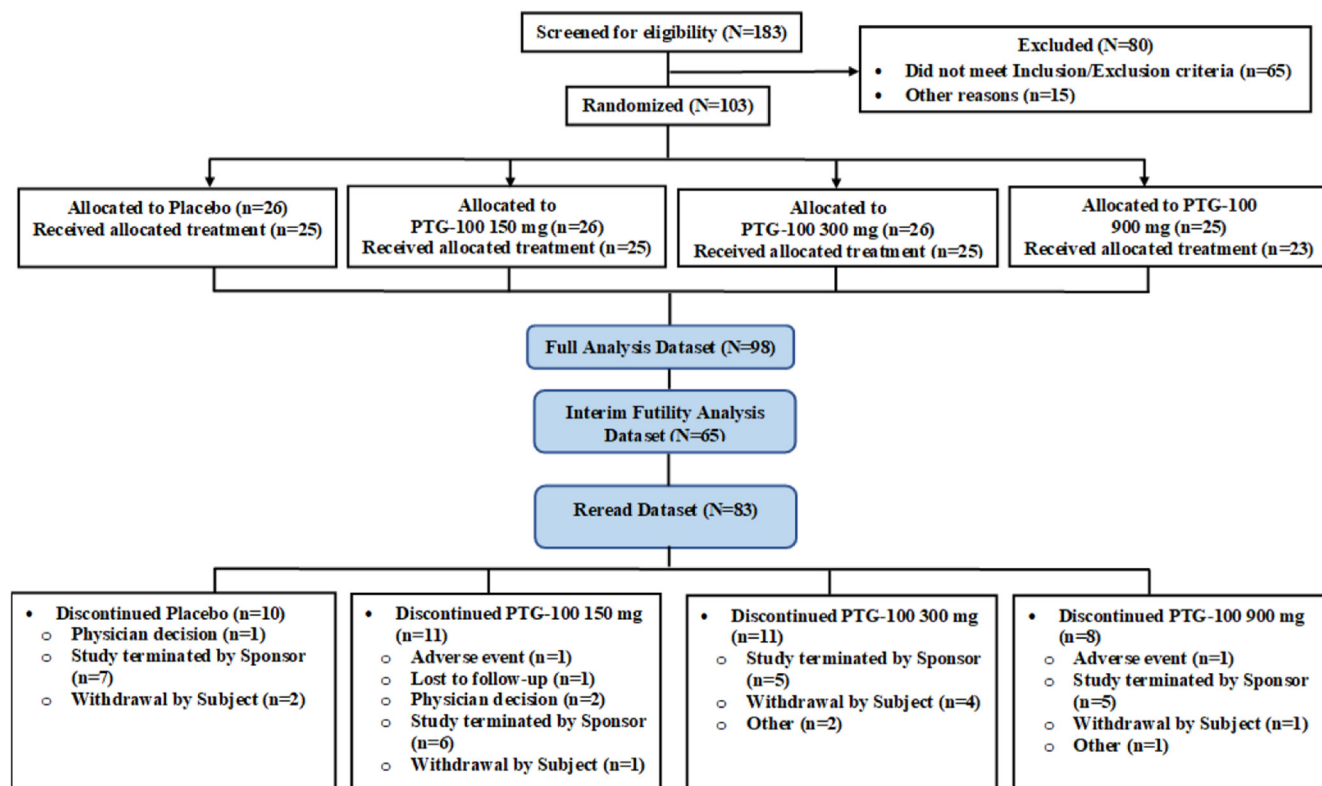
Supplementary Figure 6. C57BL/6 mice were orally dosed with PTG-100 for 14 days (5 animals/group). After the day 14 morning dose, whole blood was collected at 4, 12, and 24 hours postdose for flow cytometry analysis. Shown are the (A) percentage of RO and (B) expression of $\alpha 4\beta 7$ integrin of CD4⁺ effector memory $\alpha 4\beta 7^{+}$ T cells. The values above the bars indicate the percentage of RO or percent decrease of $\alpha 4\beta 7$ expression relative to vehicle controls. BID, twice a day.



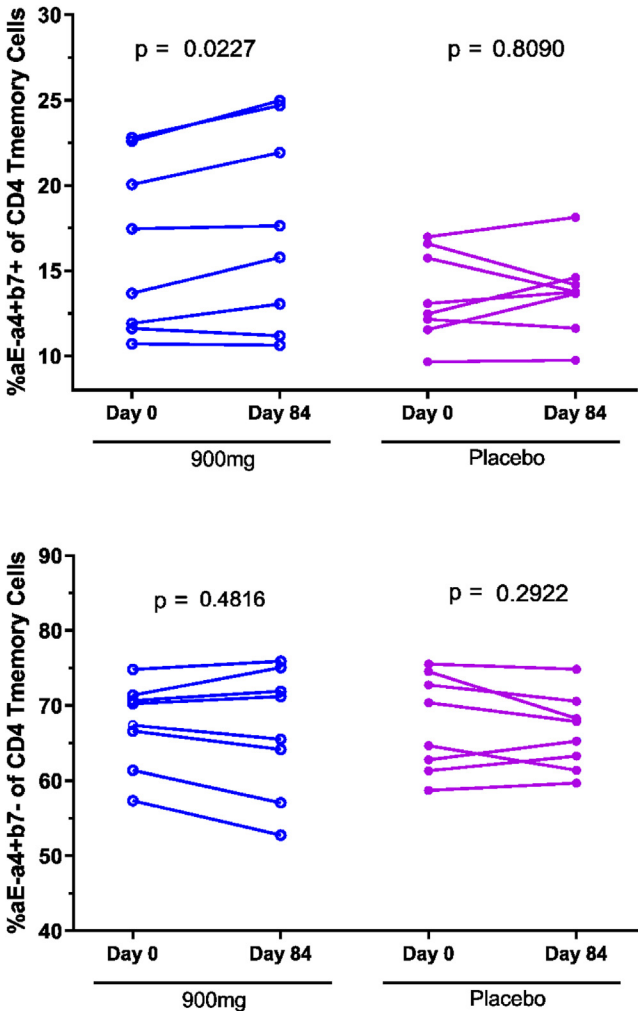
Supplementary Figure 7. Number of $\beta 7^{+}$ cells in the lesions of the distal colon of colitis mice treated with DSS for 16 days. PTG-100 dose units are mg/kg/day. DATK32 was dosed 25 mg/kg, intraperitoneally, once every 3 days. Data are presented as mean + standard deviation. Statistical analysis was performed via 1-way ANOVA with the Dunnett multiple comparison test. **** $P < .0001$.



Supplementary Figure 8. PD effects on day 1 and day 14 after once-daily dosing of PTG-100. (A) RO and (B) $\alpha 4\beta 7$ RE on $CD4^{+}\alpha 4\beta 7^{+}$ T memory cells.



Supplementary Figure 9. Patient disposition diagram.



Supplementary Figure 10. Percentage of circulating CD4⁺ T memory cells compared to placebo for (A) αE⁻α4⁺β7⁺ and (B) αE⁻α4⁺β7⁻ cells at day 0 and day 84 of dosing. Statistical significance was assessed by paired *t* test.

Supplementary Table 1. Potency of PTG-100 for Memory T Cells Isolated From Human PBMC Donors (n = 7)

Integrin	α4β7	α4β1	αLβ2
Ligand	MAdCAM-1	VCAM-1	ICAM-1
IC ₅₀ , nmol/L, mean ± SD (number of donors)	1.7 ± 0.8 (5)	>100,000 (1)	>100,000 (1)

ICAM-1, intercellular adhesion molecule-1; SD, standard deviation; VCAM-1, vascular cell adhesion molecule-1.

Supplementary Table 2. Summary of Surface Plasmon Resonance Binding Rate Constants for PTG-100-Biotin and Vedolizumab-Biotin

Reagent	k_a , (mol/L) ⁻¹ , s ⁻¹	k_d , s ⁻¹	Half-life for dissociation, minutes	K_D , nmol/L
PTG-100-biotin (PN-10941)	1120	0.0000173	667	15.4
Vedolizumab-biotin	4469	0.000266	43	59.5

NOTE. Half-life of dissociation $t_{1/2}$ (seconds) = $\ln 2/K_d$. k_a , rate of association; k_d , rate of dissociation; K_D , equilibrium dissociation constant.

Supplementary Table 3. Binding Specificity of Vedolizumab Ax647 or PTG-100 Ax647 (1 nmol/L each) in Human Whole Blood

Variable	Positive Staining, ^a %	
	Vedolizumab	PTG-100
CD4 naive T cells	55	51
CD4 memory T cells	22	20
CD8 naive T cells	53	52
CD8 memory T cells	36	36
CD19 ⁺ B cells	85	78
NK cells CD16 ⁺ 56 ⁺	42	45
Basophils	86	87
Monocytes	7	7
Eosinophils	91	92
Neutrophils	0.45	0.35

NK, natural killer.
^aPercent positive staining was determined from the gatings for fluorescence-minus-1 control for vedolizumab and PTG-100.

Supplementary Table 4. In Vitro Stability of 20 $\mu\text{mol/L}$ PTG-100 in GI Fluids of Rats, Pigs, and Humans in Rat Plasma, Rat Liver S9, and Human Intestinal S9

Species	Biological Matrix	Last Incubation Timepoint, <i>h</i> , and Number of Replicates	PTG-100 Remaining at Last Time Point, %
Rat	Intestinal fluid	5; <i>n</i> = 2	97
	Colonic fluid	6; <i>n</i> = 2	102
	Intestinal mucosa	6; <i>n</i> = 2	100
	Colonic mucosa	6; <i>n</i> = 2	123
	Plasma	6; <i>n</i> = 2	70
	Liver S9	6; <i>n</i> = 2	109
Pig	Simulated intestinal fluid	24; <i>n</i> = 5	14
	Simulated gastric fluid	6; <i>n</i> = 2	96
Human	Intestinal fluid	24; <i>n</i> = 1	116
	Intestinal S9	1; <i>n</i> = 1	99

S9, externally added metabolic activating system.

Supplementary Table 6. Summary of Phase 1 Single-Dose PK of PTG-100 (*n* = 24 participants)

PTG-100 Dose	<i>n</i>	C_{max} , <i>ng/mL</i>	T_{max} , <i>h</i> , median (range)	AUC_t , <i>ng·h/mL</i>	$t_{1/2}$, <i>h</i>
100 mg	8	2.83 ± 1.3	1.0 (0–4)	16.2 ± 9.2	3.1 ± 0.2^a
300 mg	8	7.15 ± 5.5	3.0 (1–4)	47.1 ± 29	4.3 ± 1.3^b
1000 mg	8	22.1 ± 9.5	3.0 (1–8)	198 ± 80	5.9 ± 1.7

^a*n* = 2.

^b*n* = 5.

Supplementary Table 5. PTG-100 Exposure After 30 mg/kg Single Oral Administration in Healthy C57BL/6 Mouse

GI Location	C_{max} , <i>nmol/L</i>	AUC , $\mu\text{g} \cdot \text{h/mL}$
Small intestine	16,629	43
Colon	1156	20
Peyer's patch	21,964	63
MLNs	108	0.73
Plasma	35	0.13

Supplementary Table 7. Comparison of Healthy Human Data to Healthy Mouse Data After Multiple Dosings

Species and Dose	Increase in Receptor Occupancy at 12 h, %	Increase in Receptor Occupancy at 24 h, %	Decrease in Receptor Expression at 12 h, %	Decrease in Receptor Expression at 24 h, %
Healthy mice at 50 mg/kg/day	38	8	27	18
Healthy humans at 300 mg/day	43	26	30	26

Supplementary Table 8. Overall Summary of Efficacy
Endoscopy Original Read

PTG-100 dose, mg	Clinical Remission, n/total (%)	Endoscopic Improvement, ^a n/total (%)
150	1/16 (6)	1/16 (6)
300	2/16 (13)	2/16 (13)
900	3/16 (19)	4/16 (25)
Placebo	4/17 (24)	4/17 (24)

NOTE. Interim analysis data set; m = 65 participants.
^aDefined as an endoscopic subscore of 0 or 1 of the Mayo score.

Supplementary Table 9. Overall Summary of Efficacy
Endoscopy Reread

PTG-100 Dose, mg	Clinical Remission, n/total (%)	Endoscopic Improvement, ^a n/total (%)
150	1/16 (6)	1/16 (6)
300	2/16 (13)	2/16 (13)
900	3/16 (19)	3/16 (19)
Placebo	1/17 (6)	1/17 (6)

NOTE. Interim analysis data set; n = 65 participants.
^aDefined as an endoscopic subscore of 0 or 1 of the Mayo score.